

Chiral and trace anomalies in deeply virtual Compton scattering.

II. QCD factorization and beyond

Shohini Bhattacharya^{1,*}, Yoshitaka Hatta^{2,1,†} and Werner Vogelsang^{3,‡}

¹*RIKEN BNL Research Center, Brookhaven National Laboratory, Upton, New York 11973, USA*

²*Physics Department, Brookhaven National Laboratory, Upton, New York 11973, USA*

³*Institute for Theoretical Physics, Tübingen University,
Auf der Morgenstelle 14, 72076 Tübingen, Germany*



(Received 24 May 2023; accepted 10 July 2023; published 24 July 2023)

We extend the discussion of the recently discovered “anomaly poles” in QCD Compton scattering. We perform the complete one-loop calculation of the Compton amplitude using momentum transfer t as the regulator of collinear divergences. In the gluon channel, we confirm the presence of poles $1/t$ in both the real and the imaginary parts of the amplitude. In the quark channel, we find unexpected infrared single $1/\epsilon$ and double $1/\epsilon^2$ poles. We then perform the one-loop calculation of the leading-twist quark generalized parton distributions (GPDs) for quark and gluon external states with the same regulators and find that all these singular terms can be systematically absorbed into the GPDs, showing that QCD factorization is restored to this order. Having established this, we discuss the fate of the $1/t$ poles. We argue that they become the nonperturbative building blocks of GPDs that encode the chiral and trace anomalies of QCD, in a way consistent with the known constraints these anomalies impose on the nucleon axial and gravitational form factors. The scope of research on GPDs can therefore be expanded to address the manifestation and implications of quantum anomalies in high-energy exclusive processes.

DOI: [10.1103/PhysRevD.108.014029](https://doi.org/10.1103/PhysRevD.108.014029)

I. INTRODUCTION

The past several years have witnessed significant progress in the higher-order calculation of deeply virtual Compton scattering (DVCS). In the flavor-nonsinglet channel, the three-loop evolution equation for the generalized parton distributions (GPDs) has been derived [1] together with the two-loop coefficient functions [2]. In the flavor-singlet channel, the two-loop coefficient functions for DVCS have recently been calculated [3] and even higher-order resummation effects have been studied [4]. These developments are on a steady path toward achieving the next-to-next-to-leading order accuracy in DVCS that is required for precision GPD studies at the future Electron-Ion Collider (EIC) [5].

Meanwhile, in a previous paper [6], we have explored a new approach to compute the NLO corrections in DVCS, following an earlier suggestion in polarized deep inelastic scattering (DIS) [7,8]. The key ingredient is to use momentum

transfer $t = (P_1 - P_2)^2$ as an infrared cutoff to regulate the collinear divergence, instead of the usual dimensional regularization. Previously in the calculation of the Compton amplitude in the Bjorken limit, the variable t had always been neglected when computing partonic amplitudes. Naively, one would expect that the only new effect of introducing nonzero t would be to generate higher twist corrections of order $|t|/Q^2 \ll 1$ where Q^2 is the photon virtuality. However, our explicit calculations with nonzero t have revealed “anomaly poles” $1/t$ which had not been detected in the previous calculations performed at $t = 0$ [9–13], but are consistent with the result in [7]. Moreover, these poles are accompanied by certain twist-four GPDs but without an expected suppression factor $1/Q^2$. (Rather, $1/Q^2$ has been replaced by $1/t$.) In fact, they can be interpreted as the manifestations of the QCD chiral [7,8,14] and trace [6] anomalies in high-energy scattering. The finding thus points toward a novel connection between the study of GPDs and phenomena associated with quantum anomalies such as chiral symmetry breaking and confinement.

At face value, the emergence of poles is in apparent contradiction with the QCD factorization theorem [9,15] which states that the QCD Compton scattering amplitude factorizes into the perturbatively calculable coefficient functions and the nonperturbative twist-two GPDs up to higher-twist corrections of order $1/Q^2$. However, we have already suggested in [6] that the poles found in the one-loop

*sbhattach@bnl.gov

†yhatta@bnl.gov

‡werner.vogelsang@uni-tuebingen.de

Published by the American Physical Society under the terms of the Creative Commons Attribution 4.0 International license. Further distribution of this work must maintain attribution to the author(s) and the published article's title, journal citation, and DOI. Funded by SCOAP³.

calculation may be absorbed into the twist-two GPDs as a part of the infrared subtraction procedure. The purpose of this paper is to fully demonstrate that this is indeed the case. We first perform a complete calculation of the Compton amplitude with nonzero t at one loop, in both the quark and the gluon channels, in both the polarized and the unpolarized sectors, and for the real and the imaginary parts of the amplitude. (In [6], we only calculated the imaginary part in the gluon channel.) In the gluon channel, we find $1/t$ poles also in the real part. Surprisingly, in the quark channel, we find uncanceled infrared single $1/\epsilon$ and double $1/\epsilon^2$ poles. We next perform the corresponding one-loop calculation of the unpolarized and polarized quark GPDs for free quark and gluon external states at finite t and show that all the singular terms can be systematically absorbed.

Therefore, at least to one loop, the emergence of $1/t$ poles does not contradict the QCD factorization theorem. The calculation with nonzero t may be regarded as an alternative factorization scheme. Having established this, we shift our focus to the fate of the $1/t$ poles absorbed into the twist-two GPDs. It is well known that the chiral and trace anomalies impose constraints on the nucleon axial and gravitational form factors, respectively. Since these form factors are certain moments of the twist-two GPDs, there must be corresponding constraints directly on GPDs [6]. A preliminary discussion of this has already been presented in [6]. Our extended treatment here will lend more support to the idea that this new scheme can uniquely address such profound aspects of QCD in GPD studies.

II. COMPTON SCATTERING

The amplitude for QCD Compton scattering off a proton target, $\gamma^*(q_1)p(P_1) \rightarrow \gamma^*(q_2)p(P_2)$, is given by

$$T^{\mu\nu} = i \int d^4y e^{iq \cdot y} \langle P_2 | T \{ j^\mu(y/2) j^\nu(-y/2) \} | P_1 \rangle, \quad (1)$$

where $j^\mu = \sum_q e_q \bar{\psi}_q \gamma^\mu \psi_q$ is the electromagnetic current and $q^\mu = \frac{q_1^\mu + q_2^\mu}{2}$ is the average of the incoming and outgoing photon momenta. The momentum transfer is denoted as $t = l^2$ where $l^\mu = P_2^\mu - P_1^\mu = q_1^\mu - q_2^\mu$. We introduce the

generalized Bjorken variable x_B and the skewness parameter ξ ,

$$x_B = \frac{Q^2}{2P \cdot q}, \quad \xi = \frac{q_2^2 - q_1^2}{2P \cdot q} \approx -\frac{l^+}{2P^+}, \quad (2)$$

where $Q^2 = -q^2$ is the photon virtuality and $P^\mu = \frac{P_1^\mu + P_2^\mu}{2}$. In DVCS, $q_2^2 = 0$ and $x_B \approx \xi$, but we shall keep general x_B and ξ throughout the paper.

In the generalized Bjorken limit $Q^2, 2P \cdot q \rightarrow \infty$ with x_B, t fixed and $Q^2 \gg |t|$, the Compton amplitude can be expanded as [16,17]

$$T^{\mu\nu} = \frac{g_\perp^{\mu\nu}}{2P^+} \bar{u}(P_2) \left[\gamma^+ \mathcal{H} + \frac{i\sigma^{+\nu} l_\nu}{2M} \mathcal{E} \right] u(P_2) - i \frac{\epsilon_\perp^{\mu\nu}}{2P^+} \bar{u}(P_2) \left[\gamma^+ \gamma_5 \tilde{\mathcal{H}} + \frac{\gamma_5 l^+}{2M} \tilde{\mathcal{E}} \right] u(P_2) + \dots, \quad (3)$$

where M is the proton mass. $g_\perp^{\mu\nu}$ and $\epsilon_\perp^{\mu\nu}$ are transverse projectors such that $g_\perp^{ij} = -\delta^{ij}$ and $\epsilon_\perp^{ij} = \epsilon^{ij}$ for transverse indices $i, j = 1, 2$ and the other components are zero. Our convention is $\gamma_5 = i\gamma^0\gamma^1\gamma^2\gamma^3$ and $\epsilon^{0123} = \epsilon^{-+12} = \epsilon^{12} = 1$. The ellipses in (3) stand for the contributions from the (generalized) longitudinal structure function and the so-called gluon transversity GPD. As observed in [6], they are not sensitive to anomalies and are thus left for future work.

According to QCD factorization, the Compton form factors $\mathcal{H}, \mathcal{E}, \tilde{\mathcal{H}},$ and $\tilde{\mathcal{E}}$ can be written as convolutions of nonperturbative GPDs and partonic hard-scattering amplitudes. The latter are commonly calculated in dimensional regularization in $d = 4 - 2\epsilon$ dimensions, with ϵ regularizing both ultraviolet (UV) and infrared (IR) divergences. We shall also work in d dimensions, since individual diagrams contain UV divergences. But we regularize the collinear singularity by introducing the physical variable t at the partonic level. Such a calculation is safely justified when $\sqrt{|t|} \gg \Lambda_{\text{QCD}}$ (still keeping $Q \gg \sqrt{|t|}$),¹ but we shall eventually be interested in the region $\sqrt{|t|} \sim \Lambda_{\text{QCD}}$. The result of the one-loop calculation can be summarized in the form

$$\begin{aligned} \begin{pmatrix} \mathcal{H}(x_B, \xi, t) \\ \mathcal{E}(x_B, \xi, t) \end{pmatrix} &= \sum_q e_q^2 \int_0^1 dx \left[\left(C_0(x, x_B) + \frac{\alpha_s}{2\pi} C_1^q(x, x_B, \xi) \right) \begin{pmatrix} H_q(x, \xi, t) - H_q(-x, \xi, t) \\ E_q(x, \xi, t) - E_q(-x, \xi, t) \end{pmatrix} \right. \\ &\quad \left. + \frac{\alpha_s}{2\pi} C_1^g(x, x_B, \xi) \begin{pmatrix} H_g(x, \xi, t) \\ E_g(x, \xi, t) \end{pmatrix} + \frac{\alpha_s M^2}{2\pi t} A(x, x_B, \xi) \begin{pmatrix} \mathcal{F}(x, \xi, t) \\ -\mathcal{F}(x, \xi, t) \end{pmatrix} \right] \\ &\quad + \mathcal{O}(1/Q^2) + \mathcal{O}(\alpha_s^2), \end{aligned} \quad (4)$$

¹We consider large but finite $\sqrt{|t|}$, so we are still in the generalized Bjorken limit $|t| \ll Q^2 \rightarrow \infty$ and the usual factorization in terms of the twist-two GPDs is expected. This is different from so-called wide angle Compton scattering (see, e.g., [18]) where $Q = 0$ and $s \sim -t \sim -u$. In our calculation, $s \sim Q^2$ and we systematically neglect terms of order $t/Q^2 \sim t/s$.

$$\begin{aligned} \begin{pmatrix} \tilde{H}(x_B, \xi, t) \\ \tilde{E}(x_B, \xi, t) \end{pmatrix} &= \sum_q e_q^2 \int_0^1 dx \left[\left(\tilde{C}_0(x, x_B) + \frac{\alpha_s}{2\pi} \tilde{C}_1^q(x, x_B, \xi) \right) \begin{pmatrix} \tilde{H}_q(x, \xi, t) + \tilde{H}_q(-x, \xi, t) \\ \tilde{E}_q(x, \xi, t) + \tilde{E}_q(-x, \xi, t) \end{pmatrix} \right. \\ &\quad \left. + \frac{\alpha_s}{2\pi} \tilde{C}_1^g(x, x_B, \xi) \begin{pmatrix} \tilde{H}_g(x, \xi, t) \\ \tilde{E}_g(x, \xi, t) \end{pmatrix} + \frac{\alpha_s M^2}{2\pi t} \tilde{A}(x, x_B, \xi) \begin{pmatrix} 0 \\ \tilde{\mathcal{F}}(x, \xi, t) \end{pmatrix} \right] + \mathcal{O}(1/Q^2) + \mathcal{O}(\alpha_s^2), \end{aligned} \quad (5)$$

where the notations for the twist-two quark and gluon GPDs $H_{q,g}$, $E_{q,g}$, $\tilde{H}_{q,g}$, $\tilde{E}_{q,g}$ are standard [16,17]. [The gluon GPDs are normalized as $H_g(x) = xG(x)$ and $\tilde{H}_g(x) = x\Delta G(x)$ in the forward limit, where G and ΔG are the unpolarized and polarized gluon PDFs.] Note that (4) and (5) are still in their “unsubtracted” forms in the sense that some of the coefficients contain divergences in the formal limit $t \rightarrow 0$. Their subtraction is rather unconventional, and to elaborate on this is one of the main objectives of our paper.

The leading-order coefficient functions are well known:

$$\begin{aligned} C_0(x, x_B) &= \frac{1}{x - x_B + i\epsilon} + \frac{1}{x + x_B - i\epsilon}, \\ \tilde{C}_0(x, x_B) &= \frac{1}{x - x_B + i\epsilon} - \frac{1}{x + x_B - i\epsilon}. \end{aligned} \quad (6)$$

The one-loop corrections, C_1^q , etc., have the following generic structure:

$$\begin{aligned} C_1^q(x, x_B, \xi) &= \frac{C_F}{x} \left(\kappa_{qq}(\hat{x}, \hat{\xi}) \ln \frac{Q^2}{-l^2} + \delta C_1^q(\hat{x}, \hat{\xi}) \right), \\ \tilde{C}_1^q(x, x_B, \xi) &= \frac{C_F}{x} \left(\tilde{\kappa}_{qq}(\hat{x}, \hat{\xi}) \ln \frac{Q^2}{-l^2} + \delta \tilde{C}_1^q(\hat{x}, \hat{\xi}) \right), \\ C_1^g(x, x_B, \xi) &= \frac{2T_R}{x^2} \left(\kappa_{qg}(\hat{x}, \hat{\xi}) \ln \frac{Q^2}{-l^2} + \delta C_1^g(\hat{x}, \hat{\xi}) \right), \\ \tilde{C}_1^g(x, x_B, \xi) &= \frac{2T_R}{x^2} \left(\tilde{\kappa}_{qg}(\hat{x}, \hat{\xi}) \ln \frac{Q^2}{-l^2} + \delta \tilde{C}_1^g(\hat{x}, \hat{\xi}) \right), \end{aligned} \quad (7)$$

$$\begin{aligned} C_1^q(x, x_B, \xi) &= \frac{C_F}{x} \left(\kappa_{qq}(\hat{x}, \hat{\xi}) \ln \frac{Q^2}{-l^2} + \delta C_1^q(\hat{x}, \hat{\xi}) \right), \\ \tilde{C}_1^q(x, x_B, \xi) &= \frac{C_F}{x} \left(\tilde{\kappa}_{qq}(\hat{x}, \hat{\xi}) \ln \frac{Q^2}{-l^2} + \delta \tilde{C}_1^q(\hat{x}, \hat{\xi}) \right), \\ C_1^g(x, x_B, \xi) &= \frac{2T_R}{x^2} \left(\kappa_{qg}(\hat{x}, \hat{\xi}) \ln \frac{Q^2}{-l^2} + \delta C_1^g(\hat{x}, \hat{\xi}) \right), \\ \tilde{C}_1^g(x, x_B, \xi) &= \frac{2T_R}{x^2} \left(\tilde{\kappa}_{qg}(\hat{x}, \hat{\xi}) \ln \frac{Q^2}{-l^2} + \delta \tilde{C}_1^g(\hat{x}, \hat{\xi}) \right), \end{aligned} \quad (8)$$

where $C_F = \frac{4}{3}$ and $T_R = \frac{1}{2}$ are the usual color factors. We have introduced the partonic variables $\hat{x} = \frac{x_B}{x}$ and $\hat{\xi} = \frac{\xi}{x}$, and we set the $\overline{\text{MS}}$ renormalization scale to be $4\pi e^{-\gamma_E} \mu^2 = Q^2$. The logarithm $\ln \frac{Q^2}{-l^2}$ originates from the collinear singularity and replaces the $-\frac{1}{\epsilon_{\text{IR}}}$ pole in the usual calculation in dimensional regularization with $t = 0$. The coefficients κ and $\tilde{\kappa}$ are fixed by the evolution equation of GPDs and must agree with the known results in the literature. On the other hand, the coefficient functions δC_1^q , $\delta \tilde{C}_1^q$, δC_1^g , and $\delta \tilde{C}_1^g$ are potentially scheme dependent. The results in the $\overline{\text{MS}}$ scheme can be found in [9–11,17]. Note that, somewhat at variance with the previous literature, we have used the reflection symmetry in x to restrict the x -integral to the region $0 < x < 1$. Namely, \tilde{C}_0 , \tilde{C}_1^q , C_1^g ,

H_g , E_g are even functions and C_0 , C_1^q , \tilde{C}_1^g , \tilde{H}_g , \tilde{E}_g are odd functions, respectively, under $x \rightarrow -x$. This is convenient for the discussion below.

Equations (4) and (5) resemble the usual structure dictated by the QCD factorization theorem except for the “anomaly pole” terms proportional to $1/t$. These poles are accompanied by the twist-four gluon GPDs \mathcal{F} and $\tilde{\mathcal{F}}$ defined as [7,19–22]

$$\begin{aligned} \mathcal{F}(x, \xi, t) &\equiv \frac{-4xP^+}{M} \int \frac{dz^-}{2\pi} e^{ixP^+z^-} \\ &\quad \times \frac{\langle P_2 | F^{\mu\nu}(-z^-/2) W F_{\mu\nu}(z^-/2) | P_1 \rangle}{\bar{u}(P_2)u(P_1)}, \end{aligned} \quad (9)$$

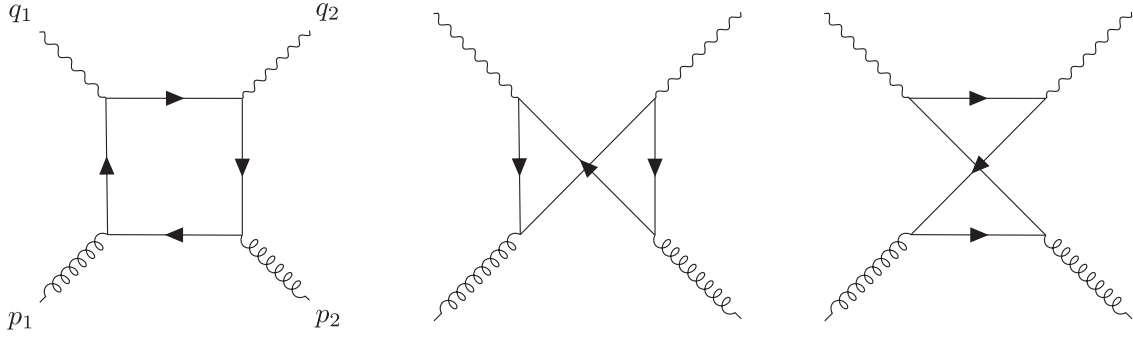
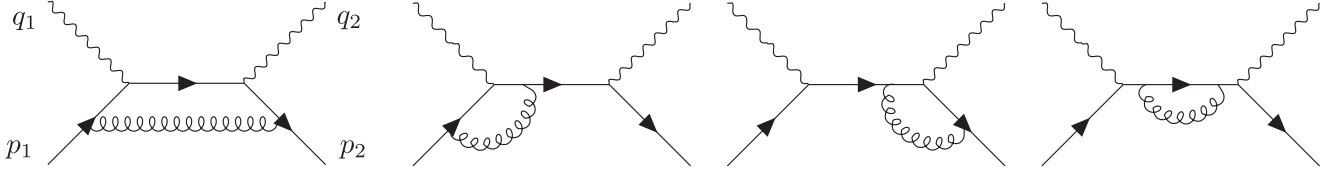
$$\begin{aligned} \tilde{\mathcal{F}}(x, \xi, t) &\equiv \frac{iP^+}{M} \int \frac{dz^-}{2\pi} e^{ixP^+z^-} \\ &\quad \times \frac{\langle P_2 | F^{\mu\nu}(-z^-/2) W \tilde{F}_{\mu\nu}(z^-/2) | P_1 \rangle}{\bar{u}(P_2)\gamma_5 u(P_1)}, \end{aligned} \quad (10)$$

where W is the straight Wilson line between $[-z^-/2, z^-/2]$. We have changed the normalization with respect to [6] in order to make these distributions dimensionless. Despite involving twist-four GPDs, these terms are not suppressed by $1/Q^2$ and apparently cause problems in the forward limit $t \rightarrow 0$. As discussed in [6] and will be further elaborated later, the emergence of poles and their fate may shed new light on the nonperturbative structure of GPDs, connecting to deep issues such as chiral symmetry breaking and the origin of hadron masses.

III. CALCULATIONS

In this section, we outline our calculation of the perturbative corrections to Compton scattering at one-loop order. The relevant Feynman diagrams for the subprocess initiated by the gluons are shown in Fig. 1, and the ones initiated by the quarks are shown in Fig. 2. For the latter case, we choose to work in Feynman gauge. (We have also worked in a general covariant gauge and confirmed that the final results are independent of the gauge as it should be.) As in Ref. [6], we parametrize the incoming and outgoing momenta as

$$q_1 = q + \frac{l}{2}, \quad q_2 = q - \frac{l}{2}, \quad p_1 = p - \frac{l}{2}, \quad p_2 = p + \frac{l}{2}. \quad (11)$$

FIG. 1. Diagrams for the subprocess $\gamma^* g \rightarrow \gamma^* g$ in Compton scattering.FIG. 2. Diagrams for the subprocess $\gamma^* q \rightarrow \gamma^* q$ in Compton scattering. Diagrams with photon lines crossed are not shown.

We also define the partonic versions of the Bjorken and skewness variables (2) as

$$\hat{x} = \frac{Q^2}{2p \cdot q} = \frac{x_B}{x}, \quad \hat{\xi} = \frac{\xi}{x} = -\hat{x} \frac{q \cdot l}{Q^2}. \quad (12)$$

The incoming and outgoing partons are assumed to be massless, $p_1^2 = p_2^2 = 0$, which leads to the conditions $p^2 = -l^2/4$ and $p \cdot l = 0$. The virtuality of the photons can be written as

$$q_1^2 = -Q^2 \frac{\hat{x} + \hat{\xi}}{\hat{x}} + \frac{l^2}{4}, \quad q_2^2 = -Q^2 \frac{\hat{x} - \hat{\xi}}{\hat{x}} + \frac{l^2}{4}. \quad (13)$$

We will abbreviate the polarization vectors for the gluons in Fig. 1 as $\epsilon^\mu(p_1) \equiv \epsilon_1^\mu$ and $\epsilon^{*\mu}(p_2) \equiv \epsilon_2^{*\mu}$.

The collinear singularity in the above diagrams will be regularized by $t = l^2$. We emphasize that, in the present ‘‘handbag’’ approximation, $t = (p_2 - p_1)^2 = (P_2 - P_1)^2$ is the same at the hadronic and partonic levels. However, we still have to work in $d = 4 - 2\epsilon$ dimensions because the individual diagrams will contain UV divergences in the real part. At the same time, working in d dimensions also helps to check if there are any leftover IR divergences that are not regularized by nonzero t alone. This point will be relevant for the quark-channel diagrams in Fig. 2. Our convention is that, if ϵ is used for the UV divergences, then $\epsilon \rightarrow \epsilon_{UV} > 0$, while if it is used for the IR divergences, then $\epsilon \rightarrow \epsilon_{IR} < 0$.

In the following, we shall refer to the two terms in (3) as the symmetric and antisymmetric parts of the Compton

amplitude, respectively. The symmetric part can be extracted with the help of the projector

$$g_{\perp}^{\mu\nu} = g^{\mu\nu} + \frac{1}{q^2(1+\gamma^2)} \left(q^\mu - \frac{q^2}{p \cdot q} p^\mu \right) \left(q^\nu - \frac{q^2}{p \cdot q} p^\nu \right) - \frac{q^\mu q^\nu}{q^2},$$

$$\gamma^2 = -\frac{p^2 q^2}{(p \cdot q)^2} = \frac{l^2 q^2}{4(p \cdot q)^2}, \quad (14)$$

such that

$$g_{\perp\mu}^\mu = d - 2 = 2(1 - \epsilon), \quad \mathcal{H}, \mathcal{E} \sim \frac{1}{2(1 - \epsilon)} g_{\perp\mu\nu}^\perp T^{\mu\nu}. \quad (15)$$

For the antisymmetric part, we use the projector $\epsilon^{\alpha\rho\mu\nu} \equiv \epsilon^{\alpha\beta\mu\nu} p_\beta$.

We evaluate the above diagrams with the help of the *Mathematica* package PACKAGE-X [23]. Below we first discuss the main features of our results specific to the gluon and quark channels. The complete results will then be presented in Sec. IV.

A. Gluon channel

Our results feature (i) a $1/l^2$ pole and (ii) a logarithm $\ln(Q^2/-l^2)$, both arising from the first and third diagrams in Fig. 1. For the symmetric case, the UV poles from the first and third diagrams add up to cancel the one arising from the second diagram. For the antisymmetric case, the UV poles from the first and third diagrams cancel. There are no leftover $1/\epsilon_{IR}$ divergences, meaning that $l^2 \neq 0$ functions as a genuine regulator of collinear divergences.

In the symmetric case, the result for the one-loop Compton scattering amplitude with external gluon polarization vectors ϵ_1, ϵ_2^* (Fig. 1) has the following generic structure:

$$\begin{aligned} & -\epsilon_1 \cdot \epsilon_2^* \left(A \ln \frac{Q^2}{-l^2} + B \right) + \frac{C}{l^2} \epsilon_1 \cdot l \epsilon_2^* \cdot l \\ & = -\epsilon_1 \cdot \epsilon_2^* \left(A \ln \frac{Q^2}{-l^2} + B - \frac{C}{2} \right) \\ & \quad + \frac{C}{l^2} \left(\epsilon_1 \cdot l \epsilon_2^* \cdot l - \frac{\epsilon_1 \cdot \epsilon_2^*}{2} l^2 \right), \end{aligned} \quad (16)$$

where A, B, C are coefficients that depend on \hat{x} and $\hat{\xi}$. In the asymmetric case, we find instead

$$i\epsilon^{ap\epsilon_2^*\epsilon_1} \left(\tilde{A} \ln \frac{Q^2}{-l^2} + \tilde{B} \right) + \tilde{C} \frac{l^\alpha}{l^2} i\epsilon^{\epsilon_1\epsilon_2^*lp}, \quad (17)$$

where $\epsilon^{\epsilon_1\epsilon_2^*lp} \equiv \epsilon^{\mu\nu\rho\lambda} \epsilon_{1\mu} \epsilon_{2\nu}^* l_\rho p_\lambda$. The first terms in (16) and (17) can be interpreted as the usual one-loop corrections to the Compton amplitude $\sim C_1^g H_g, \tilde{C}_1^g \tilde{H}_g$ through the identifications

$$\begin{aligned} -\epsilon_1 \cdot \epsilon_2^* & \sim \frac{\langle p_2 | F^{+\mu} F_\mu^+ | p_1 \rangle}{1 - \hat{\xi}^2}, \\ i\epsilon^{+p\epsilon_2^*\epsilon_1} & \sim \frac{\langle p_2 | iF^{+\mu} \tilde{F}_\mu^+ | p_1 \rangle}{1 - \hat{\xi}^2}. \end{aligned} \quad (18)$$

However, the second terms in (16) and (17) cannot be attributed to twist-two GPDs. Their structures can only arise from the twist-four operators $F^{\mu\nu} F_{\mu\nu}$ and $F^{\mu\nu} \tilde{F}_{\mu\nu}$,

$$\begin{aligned} \epsilon_1 \cdot l \epsilon_2^* \cdot l - \frac{\epsilon_1 \cdot \epsilon_2^*}{2} l^2 & \sim \langle p_2 | F^{\mu\nu} F_{\mu\nu} | p_1 \rangle, \\ 2i\epsilon^{\epsilon_1\epsilon_2^*lp} & \sim \langle p_2 | iF^{\mu\nu} \tilde{F}_{\mu\nu} | p_1 \rangle, \end{aligned} \quad (19)$$

and this is how the twist-four GPDs (9) and (10) come into play. It should be mentioned, however, that the present argument only concerns the two-parton matrix element of the operators FF and $F\tilde{F}$. Further justifications from other approaches are desirable.

B. Quark channel

In this case, our results do not contain any terms $1/l^2$. This is consistent with the expectation that the anomalies, being of purely gluonic nature, should not affect the quark sector, at least at this order. Quite unexpectedly though, we find (i) double IR poles $1/\epsilon_{\text{IR}}^2$, (ii) single IR poles $1/\epsilon_{\text{IR}}$, apart from (iii) a logarithm $\ln(Q^2/-l^2)$. Besides, we also find (iv) UV poles $1/\epsilon_{\text{UV}}$. It is interesting to discuss the origin of these poles. The UV poles arise from all the diagrams in Fig. 2 excluding the first. To cancel them, we need to include the square root of the self-energy corrections $0 = \frac{1}{\epsilon_{\text{UV}}} - \frac{1}{\epsilon_{\text{IR}}}$ on the incoming and outgoing (massless) quark lines. This converts the UV poles into single IR poles that add to the

ones in (ii). The double IR poles arise from the first diagram while the single IR poles arise from all diagrams except the fourth. It is interesting to note that, in inclusive DIS, the second and third diagrams also give rise to double poles, canceling the one from the first diagram, but in the present case they do not because the quark lines (after the reabsorption of gluons) are massive. Another interesting feature is that, in the usual $\overline{\text{MS}}$ scheme, one obtains the evolution kernel of GPDs as the coefficient of single IR poles for which all the aforementioned diagrams contribute. In our case, we reproduce the kernel as the coefficient of the logarithm (iii) for which only the first diagram contributes.

In the antisymmetric case, we project the result onto $\bar{u}(p_2)\gamma^+\gamma_5 u(p_1)$ in order to extract the twist-two component. This makes it necessary to specify the treatment of the Dirac matrix in $d \neq 4$ dimensions. We have used both the ‘naive’ fully anticommuting γ_5 and the ‘t Hooft-Veltman-Breitenlohner-Maison (HVBM) scheme [24,25]. For the latter we have computed the Dirac traces using the *Mathematica* package TRACER [26]. The HVBM scheme provides the preferred scheme [27,28] because, unlike the one with the fully anticommuting γ_5 , it is known to be algebraically consistent. Remarkably, however, in the present case the result is the same for both schemes. The reason is that all $1/\epsilon$ pole terms we find enter with a part of the Dirac trace that manifestly gives the same answer for both treatments of γ_5 . All further collinear singularities are regularized by the logarithm $\ln(Q^2/-l^2)$, so that this part of the calculation can essentially be carried out in four dimensions where, of course, both schemes coincide. The same is true for the gluonic coefficient function that has no poles in $1/\epsilon$ and can be obtained in four dimensions. Hence there are no ambiguities related to the Levi-Civita tensor being an entirely four-dimensional object. The issue of the scheme nevertheless will show up later when we discuss the one-loop calculation of the GPDs.

IV. RESULTS

A. One-loop evolution kernels

The coefficients of the logarithm $\ln(Q^2/-l^2)$ in (7) and (8) are dictated by the evolution of the twist-two GPDs and therefore must agree with the known results in the literature [9–11]. We find that this is indeed the case, meaning that the physical parameter t does the job of regularizing the collinear singularity associated with GPDs. For completeness, here we reproduce the results:

$$\begin{aligned} \kappa_{qq}(\hat{x}, \hat{\xi}) & = \frac{3}{2(1-\hat{x})} + \frac{\hat{x}^2 + 1 - 2\hat{\xi}^2}{(1-\hat{\xi}^2)(1-\hat{x})} \ln \frac{\hat{x}-1}{\hat{x}} \\ & \quad + \frac{(\hat{x}-\hat{\xi})(1-\hat{x}^2-2\hat{x}\hat{\xi}-2\hat{\xi}^2)}{(1-\hat{x}^2)\hat{\xi}(1-\hat{\xi}^2)} \ln \frac{\hat{x}-\hat{\xi}}{\hat{x}} \\ & \quad + (\hat{x} \rightarrow -\hat{x}), \end{aligned} \quad (20)$$

$$\begin{aligned} \bar{\kappa}_{qq}(\hat{x}, \hat{\xi}) &= \frac{3}{2(1-\hat{x})} + \frac{\hat{x}^2 + 1 - 2\hat{\xi}^2}{(1-\hat{\xi}^2)(1-\hat{x})} \ln \frac{\hat{x}-1}{\hat{x}} \\ &\quad - \frac{(\hat{x}-\hat{\xi})(1+\hat{x}^2+2\hat{x}\hat{\xi})}{(1-\hat{x}^2)(1-\hat{\xi}^2)} \ln \frac{\hat{x}-\hat{\xi}}{\hat{x}} \\ &\quad - (\hat{x} \rightarrow -\hat{x}), \end{aligned} \quad (21)$$

$$\begin{aligned} \kappa_{qq}(\hat{x}, \hat{\xi}) &= \frac{1-2\hat{x}+2\hat{x}^2-\hat{\xi}^2}{(1-\hat{\xi}^2)^2} \ln \frac{\hat{x}-1}{\hat{x}} \\ &\quad + \frac{(\hat{x}-\hat{\xi})(1-2\hat{\xi}\hat{x}-\hat{\xi}^2)}{\hat{\xi}(1-\hat{\xi}^2)^2} \ln \frac{\hat{x}-\hat{\xi}}{\hat{x}} \\ &\quad + (\hat{x} \rightarrow -\hat{x}), \end{aligned} \quad (22)$$

$$\begin{aligned} \bar{\kappa}_{qq}(\hat{x}, \hat{\xi}) &= \frac{2\hat{x}-1-\hat{\xi}^2}{(1-\hat{\xi}^2)^2} \ln \frac{\hat{x}-1}{\hat{x}} - 2 \frac{\hat{x}-\hat{\xi}}{(1-\hat{\xi}^2)^2} \ln \frac{\hat{x}-\hat{\xi}}{\hat{x}} \\ &\quad - (\hat{x} \rightarrow -\hat{x}), \end{aligned} \quad (23)$$

where as before $\hat{x} = \frac{x_B}{x}$, $\hat{\xi} = \frac{\xi}{x}$. Note that \hat{x} and $\hat{\xi}$ are always positive because we restricted to $0 < x < 1$ in (4) and (5). Also, an infinitesimal, negative imaginary part is understood in \hat{x} , namely, $\hat{x} \rightarrow \hat{x} - i\epsilon$ and

$$\ln(\hat{x}-1) = \ln(1-\hat{x}) - i\pi. \quad (24)$$

B. Coefficient functions

The ‘‘coefficient functions’’ in (7) and (8) are given as follows:

$$\begin{aligned} \delta C_1^q(\hat{x}, \hat{\xi}) &= -\frac{(\frac{Q^2}{\mu^2})^{\epsilon_{\text{IR}}}}{\epsilon_{\text{IR}}^2(1-\hat{x})} - \frac{3(\frac{Q^2}{\mu^2})^{\epsilon_{\text{IR}}}}{2\epsilon_{\text{IR}}(1-\hat{x})} + \frac{1-2\hat{x}-2\hat{x}^2+3\hat{\xi}^2}{2(1-\hat{x})(1-\hat{\xi}^2)} \ln \frac{\hat{x}-1}{\hat{x}} + \frac{(\hat{x}-\hat{\xi})(-1+\hat{x}^2+3\hat{x}\hat{\xi}+3\hat{\xi}^2)}{(1-\hat{x}^2)(1-\hat{\xi}^2)\hat{\xi}} \ln \frac{\hat{x}-\hat{\xi}}{\hat{x}} \\ &\quad + \frac{1+\hat{x}^2-2\hat{\xi}^2}{2(1-\hat{x})(1-\hat{\xi}^2)} \ln^2 \frac{\hat{x}-1}{\hat{x}} + \frac{\hat{x}}{2(1-\hat{\xi}^2)\hat{\xi}} \ln^2 \frac{\hat{x}-\hat{\xi}}{\hat{x}} + \frac{-1-\hat{x}^2+2\hat{\xi}^2}{2(1-\hat{x}^2)(1-\hat{\xi}^2)} \ln \frac{\hat{x}-\hat{\xi}}{\hat{x}} \ln \frac{\hat{x}+\hat{\xi}}{\hat{x}} + \frac{\pi^2-54}{12(1-\hat{x})} \\ &\quad + \frac{\hat{x}}{(1-\hat{\xi}^2)\hat{\xi}} \text{Li}_2 \frac{-2\hat{\xi}}{\hat{x}-\hat{\xi}} + \frac{1+\hat{x}^2-2\hat{\xi}^2}{(1-\hat{x})(1-\hat{\xi}^2)} \left(\text{Li}_2 \frac{1-\hat{\xi}}{1-\hat{x}} + \text{Li}_2 \frac{1+\hat{\xi}}{1-\hat{x}} \right) + (\hat{x} \rightarrow -\hat{x}), \end{aligned} \quad (25)$$

$$\begin{aligned} \delta \tilde{C}_1^q(\hat{x}, \hat{\xi}) &= -\frac{(\frac{Q^2}{\mu^2})^{\epsilon_{\text{IR}}}}{\epsilon_{\text{IR}}^2(1-\hat{x})} - \frac{3(\frac{Q^2}{\mu^2})^{\epsilon_{\text{IR}}}}{2\epsilon_{\text{IR}}(1-\hat{x})} + \frac{-1+2\hat{x}-4\hat{x}^2+3\hat{\xi}^2}{2(1-\hat{x})(1-\hat{\xi}^2)} \ln \frac{\hat{x}-1}{\hat{x}} + \frac{(\hat{x}-\hat{\xi})(1+2\hat{x}^2+3\hat{x}\hat{\xi})}{(1-\hat{x}^2)(1-\hat{\xi}^2)} \ln \frac{\hat{x}-\hat{\xi}}{\hat{x}} \\ &\quad + \frac{1+\hat{x}^2-2\hat{\xi}^2}{2(1-\hat{x})(1-\hat{\xi}^2)} \ln^2 \frac{\hat{x}-1}{\hat{x}} + \frac{\hat{\xi}}{2(1-\hat{\xi}^2)} \ln^2 \frac{\hat{x}-\hat{\xi}}{\hat{x}} - \frac{\hat{x}(1+\hat{x}^2-2\hat{\xi}^2)}{2(1-\hat{x}^2)(1-\hat{\xi}^2)} \ln \frac{\hat{x}-\hat{\xi}}{\hat{x}} \ln \frac{\hat{x}+\hat{\xi}}{\hat{x}} + \frac{\pi^2-54}{12(1-\hat{x})} \\ &\quad + \frac{\hat{\xi}}{1-\hat{\xi}^2} \text{Li}_2 \frac{-2\hat{\xi}}{\hat{x}-\hat{\xi}} + \frac{1+\hat{x}^2-2\hat{\xi}^2}{(1-\hat{x})(1-\hat{\xi}^2)} \left(\text{Li}_2 \frac{1-\hat{\xi}}{1-\hat{x}} + \text{Li}_2 \frac{1+\hat{\xi}}{1-\hat{x}} \right) - (\hat{x} \rightarrow -\hat{x}), \end{aligned} \quad (26)$$

$$\begin{aligned} \delta C_1^q(\hat{x}, \hat{\xi}) &= -\frac{1-2\hat{x}+2\hat{x}^2-\hat{\xi}^2}{(1-\hat{\xi}^2)^2} \ln \frac{\hat{x}-1}{\hat{x}} + \frac{1-2\hat{x}+2\hat{x}^2-\hat{\xi}^2}{2(1-\hat{\xi}^2)^2} \ln^2 \frac{\hat{x}-1}{\hat{x}} \\ &\quad - \frac{(\hat{x}-\hat{\xi})(1-2\hat{x}\hat{\xi}-\hat{\xi}^2)}{\hat{\xi}(1-\hat{\xi}^2)^2} \ln \frac{\hat{x}-\hat{\xi}}{\hat{x}} + \frac{\hat{x}(1+\hat{\xi}^2)}{2\hat{\xi}(1-\hat{\xi}^2)^2} \ln^2 \frac{\hat{x}-\hat{\xi}}{\hat{x}} - \frac{1+2\hat{x}^2-\hat{\xi}^2}{2(1-\hat{\xi}^2)^2} \ln \frac{\hat{x}-\hat{\xi}}{\hat{x}} \ln \frac{\hat{x}+\hat{\xi}}{\hat{x}} \\ &\quad + \frac{\hat{x}(1+\hat{\xi}^2)}{\hat{\xi}(1-\hat{\xi}^2)^2} \text{Li}_2 \frac{-2\hat{\xi}}{\hat{x}-\hat{\xi}} + \frac{1-2\hat{x}+2\hat{x}^2-\hat{\xi}^2}{(1-\hat{\xi}^2)^2} \left(\text{Li}_2 \frac{1-\hat{\xi}}{1-\hat{x}} + \text{Li}_2 \frac{1+\hat{\xi}}{1-\hat{x}} \right) + (\hat{x} \rightarrow -\hat{x}), \end{aligned} \quad (27)$$

$$\begin{aligned} \delta \tilde{C}_1^q(\hat{x}, \hat{\xi}) &= -\frac{2\hat{x}-1-\hat{\xi}^2}{(1-\hat{\xi}^2)^2} \ln \frac{\hat{x}-1}{\hat{x}} + \frac{2\hat{x}-1-\hat{\xi}^2}{2(1-\hat{\xi}^2)^2} \ln^2 \frac{\hat{x}-1}{\hat{x}} \\ &\quad + 2 \frac{\hat{x}-\hat{\xi}}{(1-\hat{\xi}^2)^2} \ln \frac{\hat{x}-\hat{\xi}}{\hat{x}} + \frac{\hat{\xi}}{(1-\hat{\xi}^2)^2} \ln^2 \frac{\hat{x}-\hat{\xi}}{\hat{x}} - \frac{\hat{x}}{(1-\hat{\xi}^2)^2} \ln \frac{\hat{x}-\hat{\xi}}{\hat{x}} \ln \frac{\hat{x}+\hat{\xi}}{\hat{x}} \\ &\quad + \frac{2\hat{\xi}}{(1-\hat{\xi}^2)^2} \text{Li}_2 \frac{-2\hat{\xi}}{\hat{x}-\hat{\xi}} + \frac{2\hat{x}-1-\hat{\xi}^2}{(1-\hat{\xi}^2)^2} \left(\text{Li}_2 \frac{1-\hat{\xi}}{1-\hat{x}} + \text{Li}_2 \frac{1+\hat{\xi}}{1-\hat{x}} \right) - (\hat{x} \rightarrow -\hat{x}), \end{aligned} \quad (28)$$

where Li_2 is the dilogarithm function. As mentioned before, in the quark channel, we find single $1/\epsilon_{\text{IR}}$ and double $1/\epsilon_{\text{IR}}^2$ infrared poles. Note that, since $\epsilon_{\text{IR}} < 0$, $(Q^2/l^2)^{\epsilon_{\text{IR}}} \rightarrow 0$ if one takes the $l^2 \rightarrow 0$ limit first. However, if one keeps l^2 finite and expands in ϵ_{IR} , the first term $\frac{3}{2(1-\hat{x})}$ in (20) and (21) gets canceled. We discuss below how these problematic terms eventually disappear.

As we also mentioned, the result (26) is independent of the scheme for γ_5 .

C. Anomaly pole terms

The coefficients of the ‘‘anomaly poles’’ $1/t$ in (4) and (5) are found to be

$$A(x, x_B, \xi) = \frac{2T_R}{x} \left(1 + \frac{\hat{x}(1-\hat{x}) \ln \frac{\hat{x}-1}{\hat{x}} + \hat{x}(\hat{x}-\hat{\xi}) \ln \frac{\hat{x}-\hat{\xi}}{\hat{x}} + (\hat{x} \rightarrow -\hat{x})}{1-\hat{\xi}^2} \right), \quad (29)$$

$$\tilde{A}(x, x_B, \xi) = \frac{8T_R}{x} \frac{(1-\hat{x}) \ln \frac{\hat{x}-1}{x} + (\hat{x}-\hat{\xi}) \ln \frac{\hat{x}-\hat{\xi}}{\hat{x}} - (\hat{x} \rightarrow -\hat{x})}{1-\hat{\xi}^2}. \quad (30)$$

The imaginary parts of these expressions agree with our results in [6]. Clearly, there are $1/t$ poles also in the real part of the Compton amplitude.² While (29) and (30) look unfamiliar and complicated, remarkably the x -integrals in (4) and (5) can be exactly rewritten in the following form:

$$\begin{aligned} \int_0^1 dx A(x, x_B, \xi) \mathcal{F}(x, \xi, t) &= 2T_R \int_0^1 dx C_0(x, x_B) \left[\int_x^1 \frac{dx'}{x'} K\left(\frac{x}{x'}, \frac{\xi}{x'}\right) \mathcal{F}(x', \xi, t) - \theta(\xi-x) \int_0^1 \frac{dx'}{x'} L\left(\frac{x}{x'}, \frac{\xi}{x'}\right) \mathcal{F}(x', \xi, t) \right] \\ &\equiv 2T_R \int_0^1 dx C_0(x, x_B) C^{\text{anom}} \otimes \mathcal{F}(x, \xi, t), \end{aligned} \quad (31)$$

$$\begin{aligned} \int_0^1 dx \tilde{A}(x, x_B, \xi) \tilde{\mathcal{F}}(x, \xi, t) &= 2T_R \int_0^1 dx \tilde{C}_0(x, x_B) \left[\int_x^1 \frac{dx'}{x'} \tilde{K}\left(\frac{x}{x'}, \frac{\xi}{x'}\right) \tilde{\mathcal{F}}(x', \xi, t) - \theta(\xi-x) \int_0^1 \frac{dx'}{x'} \tilde{L}\left(\frac{x}{x'}, \frac{\xi}{x'}\right) \tilde{\mathcal{F}}(x', \xi, t) \right] \\ &\equiv 2T_R \int_0^1 dx \tilde{C}_0(x, x_B) \tilde{C}^{\text{anom}} \otimes \tilde{\mathcal{F}}(x, \xi, t), \end{aligned} \quad (32)$$

where

$$K(x, \xi) = \frac{x(1-x)}{1-\xi^2}, \quad L(x, \xi) = \frac{x(\xi-x)}{1-\xi^2}, \quad (33)$$

$$\tilde{K}(x, \xi) = \frac{4(1-x)}{1-\xi^2}, \quad \tilde{L}(x, \xi) = \frac{4(\xi-x)}{1-\xi^2}. \quad (34)$$

That is, the leading-order kernels C_0 and \tilde{C}_0 can be factored out. The resulting convolution $C^{\text{anom}} \otimes \mathcal{F}$ agrees with what was anticipated in [6] following the general argument in [29] where actually the same integral (31) can be found. We now have the corresponding result with $\xi \neq 0$ in the polarized sector. As mentioned already in [6], the two terms in C^{anom} and \tilde{C}^{anom} come from the first and third diagrams in Fig. 1. The latter is nonzero only when the outgoing photon becomes timelike, $q_2^2 > 0$; see (13).

The identities (31) and (32) guarantee that, if the $1/t$ poles are canceled in the imaginary part of the Compton amplitude [6], the same cancellation automatically occurs in the real part as well.

V. GPD AT ONE LOOP

We have seen that the Compton scattering amplitudes at one loop contain three types of singular behaviors: (i) logarithms $\ln(-t)$, (ii) anomaly poles $1/t$, and (iii) single $1/\epsilon$ and double $1/\epsilon^2$ infrared poles (only in the quark channel). The logarithms are as expected, but the other two are unusual and potentially cause problems with factorization. We now demonstrate that all these singular structures can be absorbed into the quark GPDs in the leading-order terms of (4) and (5). Specifically, we compute the unpolarized and polarized quark GPDs³

²In Ref. [6] we computed only the imaginary part of the Compton amplitude by directly extracting the discontinuity across the variables $s = (p+q)^2$ and q_2^2 . In this paper, we compute the full amplitude. We have checked that the imaginary parts of (29), (30), and all the other results in this paper are consistent with the corresponding results in [6].

³The variables x and ξ in this section (and also in the Appendix) should better be written as \hat{x} and $\hat{\xi}$ to be more consistent with the notation in the previous sections. We, however, abbreviate $\hat{x}, \hat{\xi} \rightarrow x, \xi$ for simplicity.

$$f_q(x, \xi, t) = \int \frac{dz^-}{4\pi} e^{ixP^+z^-} \langle p_2 | \bar{q}(-z/2) W \gamma^+ q(z^-/2) | p_1 \rangle, \quad 4 \frac{1-x}{1-\xi^2}. \quad (39)$$

$$\tilde{f}_q(x, \xi, t) = \int \frac{dz^-}{4\pi} e^{ixP^+z^-} \langle p_2 | \bar{q}(-z/2) W \gamma^+ \gamma_5 q(z^-/2) | p_1 \rangle, \quad (36)$$

to one loop for on-shell $p_1^2 = p_2^2 = 0$ quark and gluon external states, keeping $t = (p_2 - p_1)^2 \neq 0$. We need to separately consider the Dokshitzer-Gribov-Lipatov-Altarelli-Parisi (DGLAP) region $0 < \xi < x \leq 1$ and the Efremov-Radyushkin-Brodsky-Lepage (ERBL) region $0 < x < \xi$ [16]. We work in $d = 4 - 2\epsilon$ dimensions to regularize the UV divergences and any leftover IR divergences. As before, they are distinguished by $1/\epsilon_{UV}$ and $1/\epsilon_{IR}$, respectively. The $\overline{\text{MS}}$ scale is denoted by $\tilde{\mu}^2 = 4\pi e^{-\gamma_E} \mu^2$.

A. Quark matrix element

The divergent part of the quark matrix element in the DGLAP region $\xi < x < 1$ is, omitting the common prefactor $\frac{\alpha_s C_F}{4\pi p^+} \bar{u}(p_2) \gamma^+ u(p_1)$ or $\frac{\alpha_s C_F}{4\pi p^+} \bar{u}(p_2) \gamma^+ \gamma_5 u(p_1)$,

$$\frac{(\tilde{\mu}^2)^\epsilon}{\epsilon_{UV}} \left[\frac{1+x^2-2\xi^2}{(1-\xi^2)(1-x)_+} + \left(\frac{3}{2} - \ln(1-\xi^2) \right) \delta(1-x) \right] - \delta(1-x) \left(\frac{1}{\epsilon_{IR}^2} + \frac{3}{2\epsilon_{IR}} \right) \left(\frac{\tilde{\mu}^2}{-l^2} \right)^\epsilon. \quad (37)$$

The derivation is outlined in the Appendix. The same result holds for both the unpolarized and the polarized GPDs. Note the double and single infrared poles. Similar ‘‘Sudakov’’ double poles have been previously encountered in the one-loop gluon matrix element of the twist-four GPDs (9) and (10) [21,22]. After convoluting with C_0 and \tilde{C}_0 , which can be done trivially using the delta function $\delta(1-x)$, they exactly match the double and single poles in (25) and (26). In other words, the poles in (25) and (26) can be absorbed into the GPDs. The finite terms are given by

$$-\frac{1+x^2-2\xi^2}{1-\xi^2} \left(\frac{\ln \frac{(1-x)^2}{1-\xi^2}}{1-x} \right)_+ - \frac{1-x}{1-\xi^2} - \frac{1}{2} \delta(1-x) \left(\ln^2(1-\xi^2) - \frac{\pi^2}{6} \right) \quad (38)$$

in the unpolarized case. In the polarized case, interestingly the result depends on the scheme for γ_5 in contrast to what we observed with the coefficient function (26). If one uses the ‘‘fully anticommuting γ_5 ,’’ the result is the same as (38). If, on the other hand, one uses the HVBM scheme, one finds an additional term

The $\mathcal{O}(\epsilon)$ difference between the two schemes now leaves a finite contribution because of the presence of the UV pole $1/\epsilon_{UV}$.

In the ERBL region, the divergent terms read

$$\frac{(\tilde{\mu}^2)^\epsilon}{\epsilon_{UV}} \frac{x+\xi}{(1+\xi)} \left(\frac{1}{1-x} + \frac{1}{2\xi} \right) \quad (40)$$

in both the unpolarized and the polarized cases. The finite terms are rather cumbersome. In the unpolarized case, we find

$$\frac{1}{2\xi(1-x)(1-\xi^2)} \left[(x-1)(x+\xi)(\xi+1) \ln(\xi^2-x^2) + 2\xi x^2 \ln \frac{1+\xi}{(x+\xi)(1-x)} + 2\xi^3 \ln \frac{x+\xi}{\xi-x} + 2\xi \ln \frac{(1+\xi)(\xi-x)}{1-x} + 4\xi^3 \ln \frac{1-x}{1+\xi} + 2(1-x)(x+\xi^2) \ln(2\xi) \right] - \frac{x+\xi}{2\xi(1+\xi)}, \quad (41)$$

and in the polarized case there is an additional term

$$4 \frac{x+\xi}{2\xi(1+\xi)} \quad (42)$$

in the HVBM scheme.

The coefficients of the UV pole in (37) and (40) constitute the $q \rightarrow q$ evolution kernel of the GPDs. After expanding $(\frac{\tilde{\mu}^2}{-l^2})^\epsilon = 1 + \epsilon \ln \frac{\tilde{\mu}^2}{-l^2}$ and convoluting with C_0 and \tilde{C}_0 , we recover (20) and (21). In other words, the logarithmic terms in (7) can be absorbed into the GPDs, as expected. The same comment applies to the $g \rightarrow q$ evolution kernel below.

B. Gluon matrix element, unpolarized

For the gluon matrix elements $\langle p_2 e_2 | \dots | p_1 e_1 \rangle$ of the quark GPD (35) and (36), we find it convenient to work in the light-cone gauge $\epsilon_1^+ = \epsilon_2^+ = 0$. The result for the unpolarized GPD in the DGLAP region is

$$f_q = \frac{\alpha_s T_R}{2\pi} \left[-(1-\xi^2) \epsilon_1 \cdot \epsilon_2^* \left(\frac{(\tilde{\mu}^2)^\epsilon}{\epsilon_{UV}} \frac{2x^2-2x+1-\xi^2}{(1-\xi^2)^2} - \frac{(2x^2-2x+1-\xi^2) \ln \frac{(1-x)^2}{1-\xi^2} + 2x(1-x)}{(1-\xi^2)^2} \right) - \frac{4x(1-x)}{l^2} \frac{1}{1-\xi^2} \left(\epsilon_1 \cdot l \epsilon_2^* \cdot l - \frac{l^2}{2} \epsilon_1 \cdot \epsilon_2^* \right) \right], \quad (43)$$

where we have factored out the structure that represents the twist-two GPD; see (18). Note the anomaly pole $1/l^2$ which was absent in the quark matrix elements. Its coefficient matches K in (33). [The factor of 4 is from (9).]

In the ERBL region, we find, omitting the prefactor $\frac{\alpha_s T_R}{2\pi}$,

$$-(1-\xi^2)\epsilon_1 \cdot \epsilon_2^* \frac{\left(\frac{\bar{\mu}^2}{-l^2}\right)^\epsilon (x+\xi)(1+\xi-2x)}{\epsilon_{UV} 2\xi(1+\xi)(1-\xi^2)} - \left(\epsilon_1 \cdot l \epsilon_2^* \cdot l - \frac{l^2}{2} \epsilon_1 \cdot \epsilon_2^*\right) \frac{1}{l^2} \frac{2x(x+\xi)}{\xi(1+\xi)} - (x \rightarrow -x). \quad (44)$$

The first term comes from the same ladder diagram as in (43). The $x \rightarrow -x$ term comes from a diagram in which the gluon legs are crossed. The latter contributes only in the ERBL region. The finite terms read, including the $x \rightarrow -x$ contribution,

$$-(1-\xi^2)\epsilon_1 \cdot \epsilon_2^* \frac{1}{\xi(1-\xi^2)^2} \left[-x(1+\xi^2) \ln \frac{\xi^2 - x^2}{4} - \xi(1+2x^2 - \xi^2) \ln \frac{(x+\xi)(1-x)}{(\xi-x)(1+x)} \right. \\ \left. + 2x(\xi \ln(1-x^2) - 2\xi \ln(1+\xi) + \xi^2 - \xi + (1+\xi^2) \ln \xi) \right]. \quad (45)$$

The coefficient of the anomaly pole is thus

$$\frac{1}{l^2} \left(\frac{2x(x+\xi)}{\xi(1+\xi)} - \frac{2x(x-\xi)}{\xi(1+\xi)} \right) = \frac{4}{l^2} \frac{x}{1+\xi}. \quad (46)$$

This agrees with

$$K(x, \xi) - L(x, \xi) = \frac{x}{1+\xi}, \quad (47)$$

which is the relevant linear combination in the ERBL region; see (31). These results, together with the observation (31), show that the $1/t$ pole in (4) can be absorbed into the unpolarized quark GPDs H_q and E_q in the leading order as a part of the infrared subtraction procedure.

C. Gluon matrix element, polarized

In the polarized case (36), we find

$$\tilde{f}_q = \frac{\alpha_s T_R}{2\pi} \left[(1-\xi^2) i \epsilon^{+p\epsilon_2^*\epsilon_1} \left(\frac{2x-1-\xi^2}{(1-\xi^2)^2} \left(\frac{\left(\frac{\bar{\mu}^2}{-l^2}\right)^\epsilon}{\epsilon_{UV}} - \ln \frac{(1-x)^2}{1-\xi^2} \right) - 2 \frac{1-x}{(1-\xi^2)^2} \right) + \frac{2il^+ \epsilon^{\epsilon_1 \epsilon_2^* l p}}{l^2} \frac{1-x}{1-\xi^2} \right], \quad (48)$$

in the DGLAP region. A simplified version of this result (with a different UV prescription) was already reported in [6]. The coefficient of the pole agrees with \tilde{K} in (34). Note that the pole is proportional to $l^{\mu=+}$, meaning that it contributes to a shift in the GPD \tilde{E}_q . In the ERBL region, the singular terms are, omitting the prefactor $\frac{\alpha_s T_R}{2\pi}$,

$$\frac{x+\xi}{2\xi(1+\xi)} \left((1-\xi^2) i \epsilon^{+p\epsilon_2^*\epsilon_1} \left(\frac{\left(\frac{\bar{\mu}^2}{-l^2}\right)^\epsilon}{\epsilon_{UV}} \frac{-1}{1+\xi} + \frac{2il^+ \epsilon^{\epsilon_1 \epsilon_2^* l p}}{l^2} \right) + (x \rightarrow -x) \right) \\ = (1-\xi^2) i \epsilon^{+p\epsilon_2^*\epsilon_1} \frac{\left(\frac{\bar{\mu}^2}{-l^2}\right)^\epsilon}{\epsilon_{UV}} \frac{-1}{(1+\xi)^2} + \frac{2il^+ \epsilon^{\epsilon_1 \epsilon_2^* l p}}{l^2} \frac{1}{1+\xi}, \quad (49)$$

where again the $x \rightarrow -x$ term comes from the crossed-leg diagram. The finite terms are, including the $x \rightarrow -x$ contribution,

$$(1-\xi^2) i \epsilon^{+p\epsilon_2^*\epsilon_1} \frac{1}{(1-\xi^2)^2} \left[-2\xi \ln(\xi^2 - x^2) + (1+\xi^2) \ln(1-x^2) - 2x \ln \frac{(1-x)(x+\xi)}{(1+x)(\xi-x)} \right. \\ \left. - 2(1+\xi^2) \ln(1+\xi) + 4\xi \ln(2\xi) + 2\xi - 2 \right]. \quad (50)$$

The coefficient of the UV pole $\frac{-1}{(1+\xi)^2}$ is the correct evolution kernel in the ERBL region as can be seen by taking the imaginary part of (23):

$$\frac{2x-1-\xi^2}{(1-\xi^2)^2} - \frac{2(x-\xi)}{(1-\xi^2)^2} = \frac{-1}{(1+\xi)^2}. \quad (51)$$

Again the coefficient of the anomaly pole agrees with

$$\tilde{K}(x, \xi) - \tilde{L}(x, \xi) = \frac{4}{1+\xi} \quad (52)$$

from (34). With the help of (32), we can absorb the $1/t$ pole in (5) into the polarized quark GPD \tilde{E}_q .

D. Relation to the $\overline{\text{MS}}$ scheme

We have thus shown that all the singular structures $1/t$, $\ln(-t)$, $1/\epsilon_{\text{IR}}$, and $1/\epsilon_{\text{IR}}^2$ in the “unsubtracted” expressions (4) and (5) can be systematically absorbed into the twist-two GPDs in the leading order. Since the matrix elements (35) and (36) contain nonsingular terms, one might choose to perform this subtraction also for the finite terms (25)–(28). An interesting question then arises as to whether, after such a subtraction, (25)–(28) reduce to the known coefficient functions in the $\overline{\text{MS}}$ scheme.⁴ Here we partially address this question by explicitly performing the subtraction in the imaginary part of the Compton amplitude.

Let us first consider the DGLAP region $0 < \xi < x$. For simplicity, we assume $x < 1$ to avoid the delta function $\delta(1-x)$. The imaginary part of (25) is

$$\frac{1-2x-2x^2+3\xi^2}{2(1-x)(1-\xi^2)} + \frac{1+x^2-2\xi^2}{(1-x)(1-\xi^2)} \ln \frac{1-\xi^2}{x(1-x)}, \quad (53)$$

where we used

$$\text{ImLi}_2 \frac{1 \pm \xi}{1-x+i\epsilon} = -\pi \ln \frac{1 \pm \xi}{1-x}. \quad (54)$$

On the other hand, the finite terms in the unpolarized quark GPD are, from (38),

$$-\frac{1+x^2-2\xi^2}{(1-x)(1-\xi^2)} \ln \frac{(1-x)^2}{1-\xi^2} - \frac{1-x}{1-\xi^2}. \quad (55)$$

The convolution with the leading-order kernel (6) is trivial for the imaginary part since $\text{Im}C_0 \propto \delta(1-x)$. We just need to subtract (55) from (53) to obtain

$$\begin{aligned} & \frac{1+x^2-2\xi^2}{(1-x)(1-\xi^2)} \ln \frac{1-x}{x} + \frac{3(1-2x+\xi^2)}{2(1-x)(1-\xi^2)} \\ & \rightarrow 2+x - \frac{3}{2(1-x)} + \frac{1+x^2}{1-x} \ln \frac{1-x}{x} + 1-x, \end{aligned} \quad (56)$$

where we have set $\xi = 0$ on the right-hand side. This agrees with the imaginary part of the $q \rightarrow q$ coefficient function in the $\overline{\text{MS}}$ scheme [9–13]. In particular, the right-hand side is the familiar $q \rightarrow q$ coefficient function for the F_1 structure function in DIS [30] for $x < 1$. Similarly, the imaginary part of (26) reads

$$\frac{-1+2x-4x^2+3\xi^2}{2(1-x)(1-\xi^2)} + \frac{1+x^2-2\xi^2}{(1-x)(1-\xi^2)} \ln \frac{1-\xi^2}{x(1-x)}. \quad (57)$$

The finite terms in the polarized quark PDF depend on the scheme adopted for the treatment of γ_5 . In the HVBM scheme, we find from (38) and (39)

$$-\frac{1+x^2-2\xi^2}{(1-x)(1-\xi^2)} \ln \frac{(1-x)^2}{1-\xi^2} + 3 \frac{1-x}{1-\xi^2}. \quad (58)$$

After the subtraction,

$$\begin{aligned} & \frac{-7+14x-10x^2+3\xi^2}{2(1-x)(1-\xi^2)} + \frac{1+x^2-2\xi^2}{(1-x)(1-\xi^2)} \ln \frac{1-x}{x} \\ & \rightarrow 2+x - \frac{3}{2(1-x)} + \frac{1+x^2}{1-x} \ln \frac{1-x}{x} - 4(1-x), \end{aligned} \quad (59)$$

in agreement with the $q \rightarrow q$ coefficient function for the g_1 structure function in the HVBM prescription. As was discussed in Refs. [28,31], it is necessary to subtract this term in order to avoid a conflict with helicity conservation and with the known first-order correction to the Bjorken sum rule. Incidentally, in the present case, the result obtained after this finite subtraction coincides with that found for a fully anticommuting γ_5 . Either way, instead of (59) the correct result becomes

$$\begin{aligned} & \frac{1-2x-2x^2+3\xi^2}{2(1-x)(1-\xi^2)} + \frac{1+x^2-2\xi^2}{(1-x)(1-\xi^2)} \ln \frac{1-x}{x} \\ & \rightarrow 2+x - \frac{3}{2(1-x)} + \frac{1+x^2}{1-x} \ln \frac{1-x}{x}. \end{aligned} \quad (60)$$

As for the $g \rightarrow q$ coefficients, the imaginary part of (27) is

$$\frac{1-2x+2x^2-\xi^2}{(1-\xi^2)^2} \left(\ln \frac{1-\xi^2}{x(1-x)} - 1 \right). \quad (61)$$

From this, we subtract the finite terms in (43),

⁴We thank Vladimir Braun for raising this question.

$$-\frac{1-2x+2x^2-\xi^2}{(1-\xi^2)^2} \ln \frac{(1-x)^2}{1-\xi^2} - \frac{2x(1-x)}{(1-\xi^2)^2}, \quad (62)$$

to obtain

$$\begin{aligned} & \frac{1-2x+2x^2-\xi^2}{(1-\xi^2)^2} \ln \frac{1-x}{x} + \frac{-1+4x-4x^2+\xi^2}{(1-\xi^2)^2} \\ & \rightarrow (1-2x+2x^2) \left(\ln \frac{1-x}{x} - 1 \right) + 2x(1-x). \end{aligned} \quad (63)$$

This agrees with the $g \rightarrow q$ coefficient function for the F_1 structure function in the $\overline{\text{MS}}$ scheme. Finally, the imaginary part of (28) is

$$\frac{2x-1-\xi^2}{(1-\xi^2)^2} \left(\ln \frac{1-\xi^2}{x(1-x)} - 1 \right). \quad (64)$$

Subtracting from this the finite terms in (48),

$$-\frac{2x-1-\xi^2}{(1-\xi^2)^2} \ln \frac{(1-x)^2}{1-\xi^2} - \frac{2(1-x)}{(1-\xi^2)^2}, \quad (65)$$

we find

$$\begin{aligned} & \frac{2x-1-\xi^2}{(1-\xi^2)^2} \ln \frac{1-x}{x} + \frac{3-4x+\xi^2}{(1-\xi^2)^2} \\ & \rightarrow (2x-1) \left(\ln \frac{1-x}{x} - 1 \right) + 2(1-x), \end{aligned} \quad (66)$$

in agreement with the $\overline{\text{MS}}$ $g \rightarrow q$ coefficient function for the g_1 structure function. It is interesting to recall that the last term $2(1-x) \otimes \Delta G(x)$ in (66) caused a lot of discussion (see, e.g., [32,33]) in the wake of the proton “spin crisis” in the late 1980s. In the standard $\overline{\text{MS}}$ calculation in the forward limit $t=0$, this term arises from the IR region of the loop diagram, and therefore does not seem to qualify as a part of the “hard” coefficient. In our calculation of the Compton amplitude, this term is replaced by the pole term $\frac{1}{t}(1-x) \otimes \tilde{F}(x)$ and gets absorbed into the GPD \tilde{E}_q . Nevertheless, the $2(1-x)$ term is restored after the subtraction because the polarized GPD (36) generates it from the UV region of the loop momentum. Therefore, even though the final result (66) is the same, from our perspective the term $2(1-x)$ is legitimately considered a hard contribution.

We have further performed the subtraction of the constant terms (41), (45), and (50) in the ERBL region $x < \xi$ from the imaginary part of (25)–(28) and observed consistent agreement with the $\overline{\text{MS}}$ coefficient functions [17]. We have thus partially verified that the “off-forward” regularization is equivalent to the $\overline{\text{MS}}$ scheme after the subtraction of finite terms is made. Extending this to the real part of the Compton amplitude is left for future work.

On the other hand, since the treatment of finite terms is a matter of scheme choice, one can choose to subtract only the singular terms. Equations (25)–(28), with the single and double poles omitted, are then the coefficient functions in such a scheme.

VI. IMPRINTS OF ANOMALIES ON GPD

Let us discuss the implications of our results. Superficially, it may seem as if nothing has happened in the end. After absorbing all the singular terms into the twist-two GPDs, the Compton amplitude will be given by the usual factorized form with possibly different coefficient functions due to a different scheme choice. The common attitude is that one does not care about these singular terms once they have been “discarded” into a parton distribution, as they will be taken care of by the nonperturbative QCD dynamics. One can also take the view that the $1/t$ poles should disappear in the limit $t \rightarrow 0$, because nonperturbative effects must intervene when $\sqrt{|t|} \sim \Lambda_{\text{QCD}}$. However, from the point of view of factorization, technically speaking one is allowed to choose any infrared regulator that can isolate the collinear divergences, as long as they can eventually be absorbed into parton distributions when the latter are computed with the same IR regulator. In this sense, the use of t is no different from other regulators such as the current quark mass m_q and the dimensionality $d \neq 4$. One may even argue that it is a more physical scheme, since $t \neq 0$ in actual experiments and naturally cuts off collinear divergences.

Technicalities aside, the real reason we are pursuing the off-forward calculation with nonzero t is that this approach has the potential to uncover nonperturbative connections between GPDs and QCD anomalies. Indeed, the very idea that twist-four GPDs are absorbed into twist-two GPDs is quite nonstandard and needs to be investigated further, rather than dismissed as a routine infrared subtraction procedure. This is all the more so because, as discussed in [6,8] and elaborated further below, the results we shall get are consistent with what we know about the axial and gravitational form factors that are certain moments of the twist-two GPDs.

A. Axial and gravitational form factors

1. Isovector axial form factors

To motivate our discussion, let us first recall the familiar example of the isovector axial current $J_{5a}^\alpha = \sum_q \bar{q} \gamma^\alpha \gamma_5 \frac{\tau^a}{2} q$ where $\tau^{a=1,2,3}$ are the Pauli matrices. Its nucleon matrix element is parametrized by the axial form factors

$$\langle P_2 | J_{5a}^\alpha | P_1 \rangle = \bar{u}(P_2) \left[\gamma^\alpha \gamma_5 F_A(t) + \frac{l^\alpha \gamma_5}{2M} F_P(t) \right] \frac{\tau^a}{2} u(P_1). \quad (67)$$

In QCD with $n_f = 2$ massless flavors, the current is exactly conserved, $\partial_\alpha J_{5a}^\alpha = 0$, due to chiral symmetry. This imposes a constraint among the form factors

$$2MF_A(t) + \frac{tF_P(t)}{2M} = 0. \quad (68)$$

Clearly, $F_P(t)$ has a pole at $t = 0$:

$$F_P(t) \approx \frac{-4M^2 g_A^{(3)}}{t} \quad (t \rightarrow 0), \quad (69)$$

where $g_A^{(3)} = F_A(0) \approx 1.3$ is the isovector axial coupling constant. The pole is generated by the exchange of the massless pion which is the Nambu-Goldstone boson of spontaneously broken chiral symmetry. This requirement leads to the well-known Goldberger-Treiman relation

$$g_A^{(3)} = \frac{f_\pi g_{\pi NN}}{M}, \quad (70)$$

where f_π is the pion decay constant and $g_{\pi NN}$ is the pion-nucleon coupling. Now recall that $F_P(t)$ is the first moment of the isovector GPD \tilde{E} ,

$$F_P(t) = \int_{-1}^1 dx (\tilde{E}_u(x, \xi, t) - \tilde{E}_d(x, \xi, t)). \quad (71)$$

Barring an unlikely possibility that the pole $1/t$ is generated by the x -integral, the GPDs themselves hence have a massless pole at $t = 0$:

$$\tilde{E}_u(x, \xi, t) - \tilde{E}_d(x, \xi, t) \sim \theta(\xi - |x|) \frac{g_A^{(3)}}{t} \quad (t \rightarrow 0). \quad (72)$$

Indeed, such a pole has been discussed in the GPD literature (see, e.g., [34]) where it has been argued that the pole exists only in the ERBL region $\xi > x$ where GPDs probe the mesonic degrees of freedom inside the nucleon. In actual QCD with massive quarks, the pole is shifted to the physical pion mass, $\frac{1}{t} \rightarrow \frac{1}{t - m_\pi^2}$.

2. Isoscalar axial form factors

The story is more complicated for the singlet axial current $J_5^\alpha = \sum_q \bar{q} \gamma^\alpha \gamma_5 q$. The associated form factors g_A and g_P , appearing in the nucleon matrix element via

$$\langle P_2 | J_5^\alpha | P_1 \rangle = \bar{u}(P_2) \left[\gamma^\alpha \gamma_5 g_A(t) + \frac{l^\alpha \gamma_5}{2M} g_P(t) \right] u(P_1), \quad (73)$$

are related to the flavor-singlet polarized GPDs as

$$\begin{aligned} g_A(t) &= \sum_q \int_{-1}^1 dx \tilde{H}_q(x, \xi, t) \\ &= \sum_q \int_0^1 dx (\tilde{H}_q(x, \xi, t) + \tilde{H}_q(-x, \xi, t)), \end{aligned} \quad (74)$$

$$\begin{aligned} g_P(t) &= \sum_q \int_{-1}^1 dx \tilde{E}_q(x, \xi, t) \\ &= \sum_q \int_0^1 dx (\tilde{E}_q(x, \xi, t) + \tilde{E}_q(-x, \xi, t)). \end{aligned} \quad (75)$$

In contrast to the isovector current above, J_5^α is not conserved due to the chiral $[U_A(1)]$ anomaly,

$$\partial_\alpha J_5^\alpha = -\frac{n_f \alpha_s}{4\pi} F^{\mu\nu} \tilde{F}_{\mu\nu}. \quad (76)$$

This leads to the following exact relation:

$$2M g_A(t) + \frac{t g_P(t)}{2M} = i \frac{\langle P_2 | \frac{n_f \alpha_s}{4\pi} F \tilde{F} | P_1 \rangle}{\bar{u}(P_2) \gamma_5 u(P_1)}. \quad (77)$$

We see that, in the absence of the anomaly (i.e., if the right-hand side were zero), $g_P(t)$ would have a pole at $t = 0$,

$$\frac{g_P(t)}{2M} \approx -\frac{2M \Delta \Sigma}{t} \quad (t \rightarrow 0), \quad (78)$$

where $\Delta \Sigma = g_A(0)$ is the quark helicity contribution to the nucleon spin. Such a pole can be interpreted as due to the exchange of the massless ninth Nambu-Goldstone boson, the ‘‘primordial’’ η_0 meson. Moreover, Eq. (75) suggests that already the flavor-singlet GPD $\sum_q \tilde{E}_q$ would have a pole $1/t$, just as (72).

In reality, however, the $U_A(1)$ axial symmetry is explicitly broken due to the anomaly, and $g_P(t)$ exhibits a pole at the physical η' meson mass $t = m_{\eta'}^2$. The exact mechanism behind this scenario was a great debate in the late 1970s culminating in the works of Witten [35] and Veneziano [36]. In a nutshell, η_0 acquires mass via a resummation [36]

$$\frac{1}{t} + \frac{m_{\eta'}^2}{t^2} + \frac{m_{\eta'}^4}{t^3} + \dots = \frac{1}{t - m_{\eta'}^2} = -\left(\frac{1}{t} \frac{m_{\eta'}^2}{m_{\eta'}^2 - t} - \frac{1}{t} \right), \quad (79)$$

due to its coupling with the gluonic topological fluctuations $m_{\eta'}^2 \propto \langle (F \tilde{F})^2 \rangle$. On the right-hand side, we have deliberately expressed the resulting propagator as the difference of two poles at $t = 0$. Now let us compare this with (77) which can be identically rewritten in the form

$$\begin{aligned}
\frac{g_P(t)}{2M} &= \frac{1}{t} \left(i \frac{\langle P_2 | \frac{n_f \alpha_s}{4\pi} F \tilde{F} | P_1 \rangle}{\bar{u}(P_2) \gamma_5 u(P_1)} - 2M g_A(t) \right) \\
&= \frac{1}{t} \left(i \frac{\langle P_2 | \frac{n_f \alpha_s}{4\pi} F \tilde{F} | P_1 \rangle}{\bar{u}(P_2) \gamma_5 u(P_1)} - i \frac{\langle P_2 | \frac{n_f \alpha_s}{4\pi} F \tilde{F} | P_1 \rangle}{\bar{u}(P_2) \gamma_5 u(P_1)} \Big|_{t=0} \right) \\
&\quad + 2M \frac{g_A(0) - g_A(t)}{t}. \tag{80}
\end{aligned}$$

We neglect the last term assuming $g_A(t) \approx g_A(0) = \Delta\Sigma$ to be varying only slowly with t .⁵ The right-hand side can then be interpreted as a cancellation of two poles at $t = 0$, just as (79), between the ‘‘anomaly pole’’ (first term) and the naive pole (78) from the massless η_0 meson exchange (second term). Equations (79) and (80) are actually identical in the single-pole approximation where (80) is saturated by

$$\begin{aligned}
\frac{g_P(t)}{2M} &\approx \frac{2M\Delta\Sigma}{m_{\eta'}^2 - t} \\
i \frac{\langle P_2 | \frac{n_f \alpha_s}{4\pi} F \tilde{F} | P_1 \rangle}{\bar{u}(P_2) \gamma_5 u(P_1)} &\approx 2M\Delta\Sigma \frac{m_{\eta'}^2}{m_{\eta'}^2 - t}. \tag{81}
\end{aligned}$$

In the context of polarized DIS, the cancellation of poles just described had been originally envisaged in [14] and further elaborated in [8] to resolve issues with the g_1 structure function. Compton scattering and GPDs offer a more general setup to explore the physics of the anomaly to its full extent.

3. Gravitational form factors

We now point out that one can repeat the same story for the QCD energy momentum tensor $\Theta^{\alpha\beta}$ and its nucleon matrix element that defines the gravitational form factors,

$$\begin{aligned}
\langle P_2 | \Theta^{\alpha\beta} | P_1 \rangle &= \bar{u}(P_2) \left[A(t) \frac{P^\alpha P^\beta}{M} + (A(t) + B(t)) \frac{P^{(\alpha} i \sigma^{\beta)\lambda} l_\lambda}{2M} \right. \\
&\quad \left. + D(t) \frac{l^\alpha l^\beta - g^{\alpha\beta} t}{4M} \right] u(P_1), \tag{82}
\end{aligned}$$

where $a^{(\mu} b^{\nu)} = \frac{1}{2}(a^\mu b^\nu + a^\nu b^\mu)$. Taking the trace, we find an exact constraint among the form factors:

$$\begin{aligned}
\langle P_2 | (\Theta)_\alpha^\alpha | P_1 \rangle &= M \left(A(t) + \frac{B(t)}{4M^2} t - \frac{3D(t)}{4M^2} t \right) \bar{u}(P_2) u(P_1) \\
&= \langle P_2 | \frac{\beta(g)}{2g} F^{\mu\nu} F_{\mu\nu} | P_1 \rangle. \tag{83}
\end{aligned}$$

⁵A partial justification of this comes from the large- N_c approximation where $m_{\eta'} \sim \mathcal{O}(1/\sqrt{N_c})$ is considered as small, at least parametrically, compared to the singlet axial vector meson masses $m_A \sim \mathcal{O}(N_c^0)$. Thus, as long as one is interested in the region $|t| \sim m_{\eta'}^2$, the variation of $g_A(t) \sim 1/(t - m_A^2)$ can be neglected. In practice, however, the $\eta'(957)$ is only slightly lighter than the $f_1(1285)$.

The right-hand side, on which $\beta(g)$ is the QCD beta function, is the trace anomaly that signifies the explicit breaking of conformal symmetry. If one naively neglects it, one finds a massless pole in $D(t)$ at $t = 0$:

$$\frac{3D(t)}{4} \approx \frac{M^2}{t} \quad (t \rightarrow 0), \tag{84}$$

where the conditions $A(0) = 1$ and $B(0) = 0$ have been used [so that one can omit $tB(t)$ as $t \rightarrow 0$]. By analogy with the massless η_0 pole in (78), one might interpret the pole in (84) as due to the exchange of spin-0 glueballs, which would couple to the operator $\Theta^{\alpha\beta}$ and which would have been massless in the absence of the trace anomaly [6]. In reality, however, the anomaly modifies (84) to

$$\begin{aligned}
\frac{3D(t)}{4} &\approx \frac{M^2}{t} \left(A(t) - \frac{\langle P_2 | \frac{\beta(g)}{2g} F^2 | P_1 \rangle}{M \bar{u}(P_2) u(P_1)} \right) \\
&= -\frac{M}{t} \left(\frac{\langle P_2 | \frac{\beta(g)}{2g} F^2 | P_1 \rangle}{\bar{u}(P_2) u(P_1)} - \frac{\langle P_2 | \frac{\beta(g)}{2g} F^2 | P_1 \rangle}{\bar{u}(P_2) u(P_1)} \Big|_{t=0} \right) \\
&\quad + M^2 \frac{A(t) - A(0)}{t}. \tag{85}
\end{aligned}$$

Note the similarity to (80). The $D(t)$ -form factor can be interpreted as the difference of two poles at $t = 0$, between the anomaly pole (first term in the brackets) and the naive glueball pole (84) (second term in the brackets). As a result of this cancellation, the pole in $D(t)$ is shifted from $t = 0$ to physical glueball masses $t = m_G^2$ presumably in a way similar to (79). However, unlike the situation in (80), in the present case the last term $A(t) - A(0)$ of (85), which is related to spin-2 glueballs [6], is likely important at least from the large- N_c perspective. Since the trace anomaly cannot be turned off in the large- N_c limit, the masses of 2^{++} and 0^{++} glueballs are both $\mathcal{O}(N_c^0)$. Moreover, the analysis in [37] suggests that the single pole approximation [cf. (81)] may not be a good approximation. The $D(t)$ -form factor thus exhibits ‘‘glueball dominance’’

$$D(t) = \sum_i^{0^{++}} \frac{a_i}{m_{G_i}^2 - t} + \sum_j^{2^{++}} \frac{b_j}{m_{G_j}^2 - t}, \tag{86}$$

where the two contributions come from the $\langle F^2 \rangle$ and $A(t)$ terms in (85), respectively. Incidentally, by taking the $t \rightarrow 0$ limit of (85), one finds [38]

$$\frac{3D(0)}{4} = -M \frac{d}{dt} \frac{\langle P_2 | \frac{\beta(g)}{2g} F^2 | P_1 \rangle}{\bar{u}(P_2) u(P_1)} \Big|_{t=0} + M^2 \frac{dA(t)}{dt} \Big|_{t=0}. \tag{87}$$

The slope of a form factor at $t = 0$ defines a ‘‘radius’’ of the hadron. Equation (87) shows that the D -term $D(t = 0)$ is

related to the difference between two radii, one defined by the scalar form factor $\langle F^2 \rangle$ (related to the 0^{++} glueball masses) and the other by the A -form factor (related to the 2^{++} glueball masses); see recent discussions in [37,39–41].

As we have seen in the above three examples, the existence or not of a massless pole in form factors teaches us fundamental insights into the nonperturbative dynamics of QCD. However, despite the known connections between form factors and GPDs, the corresponding discussion at the GPD level has been limited to the isovector sector (72) in the literature (see, however, [42]). Our main purpose is to extend this argument to the singlet sector.

B. Anomaly poles in GPDs

Let us now return to our context. We have argued in Sec. V that the pole $1/t$ in the one-loop Compton amplitude (5) should be absorbed into \tilde{E}_q . This means that \tilde{E}_q acquires a component related to the twist-four GPD $\tilde{\mathcal{F}}$:

$$\begin{aligned} & \sum_q (\tilde{E}_q(x, \xi, t) + \tilde{E}_q(-x, \xi, t)) \\ &= \frac{T_R n_f \alpha_s M^2}{\pi t} \tilde{\mathcal{C}}^{\text{anom}} \otimes \tilde{\mathcal{F}}(x, \xi, t) + \dots, \end{aligned} \quad (88)$$

where $\tilde{\mathcal{C}}^{\text{anom}}$ is defined in (32). Integrating over x , we exactly reproduce the first term of (80). Moreover, Eq. (80) suggests that there is another, primordial pole in \tilde{E}_q which exactly cancels the $1/t$ pole to make \tilde{E}_q finite for all values of x and ξ in the limit $t \rightarrow 0$. A simple, yet *ad hoc*, fix consistent with (80) is to add a ‘‘counterterm’’

$$\begin{aligned} & \sum_q (\tilde{E}_q(x, \xi, t) + \tilde{E}_q(-x, \xi, t)) \\ & \approx \frac{T_R n_f \alpha_s M^2}{\pi t} \tilde{\mathcal{C}}^{\text{anom}} \otimes (\tilde{\mathcal{F}}(x, \xi, t) - \tilde{\mathcal{F}}(x, \xi, 0)). \end{aligned} \quad (89)$$

This may be viewed as the nonlocal version of the local relation (80). The second added term is an analog of (72), but interestingly, in the present case the pole is not limited to the ERBL region $x < \xi$. We postulate (89) as a non-perturbative relation between the twist-two and twist-four GPDs mediated by the chiral anomaly.

The fate of the $1/t$ pole in the unpolarized sector and its connection to the trace anomaly are more involved. This is partly because the QCD energy momentum tensor consists of a quark and a gluon part, $\Theta^{\alpha\beta} = \sum_q \Theta_q^{\alpha\beta} + \Theta_g^{\alpha\beta}$, in contrast to J_5^g which is purely a quark operator. Accordingly, one can define gravitational form factors separately for quarks and gluons [43]:

$$\begin{aligned} \langle P_2 | \Theta_{q,g}^{\alpha\beta} | P_1 \rangle &= \bar{u}(P_2) \left[A_{q,g}(t) \frac{P^\alpha P^\beta}{M} \right. \\ &+ (A_{q,g}(t) + B_{q,g}(t)) \frac{P^{(\alpha} i \sigma^{\beta)\lambda} l_\lambda}{2M} \\ &+ D_{q,g}(t) \frac{l^\alpha l^\beta - g^{\alpha\beta} t}{4M} + \left. \tilde{C}_{q,g}(t) M g^{\alpha\beta} \right] u(P_1). \end{aligned} \quad (90)$$

They are related to the second moments of the unpolarized quark GPDs,

$$\begin{aligned} \int_{-1}^1 dx x H_q(x, \xi, t) &= \int_0^1 dx x (H_q(x, \xi, t) - H_q(-x, \xi, t)) \\ &= A_q(t) + \xi^2 D_q(t), \end{aligned} \quad (91)$$

$$\begin{aligned} \int_{-1}^1 dx x E_q(x, \xi, t) &= \int_0^1 dx x (E_q(x, \xi, t) - E_q(-x, \xi, t)) \\ &= B_q(t) - \xi^2 D_q(t), \end{aligned} \quad (92)$$

and similarly for the gluon GPDs. Taking the trace of (82), we find

$$\begin{aligned} & \langle P_2 | \sum_q (\Theta_q)_\alpha^\alpha | P_1 \rangle \\ &= \sum_q M \left(A_q(t) + 4\tilde{C}_q(t) + \frac{B_q(t)}{4M^2} t - \frac{3D_q(t)}{4M^2} t \right) \bar{u}(P_2) u(P_1) \\ &= \langle P_2 | \frac{\beta_q(g)}{2g} F^2 | P_1 \rangle \approx \langle P_2 | \frac{T_R n_f \alpha_s}{6\pi} F^2 | P_1 \rangle, \end{aligned} \quad (93)$$

where $\frac{\beta_q}{2g}$ is the quark part of the trace anomaly that can be systematically calculated in perturbation theory [44–47]. To lowest order, it is simply the n_f term of the beta function:

$$\begin{aligned} (\Theta_q)_\alpha^\alpha + (\Theta_g)_\alpha^\alpha &= \frac{\beta(g)}{2g} F^{\mu\nu} F_{\mu\nu} \\ &= -\frac{\alpha_s}{8\pi} \left(\frac{11N_c}{3} - \frac{4T_R n_f}{3} \right) F^2 + \dots \end{aligned} \quad (94)$$

Clearly, Eq. (93) is not as constraining as (83) because of the new form factors $B_q(t)$ and $\tilde{C}_q(t)$. [Note that $B_q(0)$, $\tilde{C}_q(0) \neq 0$ although $B_q(0) + B_g(0) = \tilde{C}_q(0) + \tilde{C}_g(0) = 0$.] Nevertheless we may try to rewrite it in a way similar to (85)

$$\begin{aligned} & \sum_q \frac{3D_q(t) - B_q(t)}{4} \\ &= -\frac{M}{t} \left(\frac{\langle P_2 | \frac{\beta_q}{2g} F^2 | P_1 \rangle}{\bar{u}(P_2) u(P_1)} - \frac{\langle P_2 | \frac{\beta_q}{2g} F^2 | P_1 \rangle}{\bar{u}(P_2) u(P_1)} \Big|_{t=0} \right) \\ &+ \frac{M^2}{t} \sum_q (A_q(t) + 4\tilde{C}_q(t) - A_q(0) - 4\tilde{C}_q(0)). \end{aligned} \quad (95)$$

Let us now discuss how the constraint (95) from the trace anomaly is encoded in the GPDs. We have argued that the anomaly poles in (4) should be absorbed into the unpolarized GPDs,

$$\begin{aligned} & \sum_q (H_q(x, \xi, t) - H_q(-x, \xi, t)) \\ &= \frac{T_R n_f \alpha_s M^2}{\pi t} C^{\text{anom}} \otimes \mathcal{F}(x, \xi, t) + \dots, \end{aligned} \quad (96)$$

$$\begin{aligned} & \sum_q (E_q(x, \xi, t) - E_q(-x, \xi, t)) \\ &= -\frac{T_R n_f \alpha_s M^2}{\pi t} C^{\text{anom}} \otimes \mathcal{F}(x, \xi, t) + \dots, \end{aligned} \quad (97)$$

where C^{anom} is defined in (31). Taking the second moment and comparing with (91), we find

$$\begin{aligned} \sum_q A_q(t) \Big|_{\text{pole}} &= -\sum_q B_q(t) \Big|_{\text{pole}} \\ &= -\frac{M \langle P_2 | \frac{T_R n_f \alpha_s}{6\pi} F^{\mu\nu} (i\overleftrightarrow{D}^+)^2 F_{\mu\nu} | P_1 \rangle}{t (P^+)^2 \bar{u}(P_2) u(P_1)}, \end{aligned} \quad (98)$$

$$\sum_q D_q(t) \Big|_{\text{pole}} = -\frac{M \langle P_2 | \frac{T_R n_f \alpha_s}{6\pi} F^2 | P_1 \rangle}{t \bar{u}(P_2) u(P_1)}. \quad (99)$$

Equation (99) seems to reproduce the first term of (95) after β_q is expanded to lowest order. However, apparently there is a factor $\frac{3}{4}$ mismatch in the normalization. Besides, the previous argument around (85) did not hint at the possible existence of an anomaly pole in the A_q, B_q form factors.

To understand these differences, we quote the one-loop result for the energy momentum tensor matrix element between on-shell gluon (not nucleon) states [48]:

$$\begin{aligned} \langle P_2 | \Theta_q^{\alpha\beta} | P_1 \rangle &= -\frac{T_R \alpha_s}{6\pi} \left(\frac{p^\alpha p^\beta}{t} + \frac{l^\alpha l^\beta - t g^{\alpha\beta}}{4t} \right) \langle P_2 | F^{\mu\nu} F_{\mu\nu} | P_1 \rangle \\ &+ \dots \end{aligned} \quad (100)$$

A superficial comparison with (90) suggests that poles of equal magnitude are induced in the A_q, B_q, D_q form factors

$$A_q(t) \approx -B_q(t) \approx D_q(t) \sim \frac{\langle \alpha_s F^2 \rangle}{t}, \quad (101)$$

and the issue of the factor $\frac{3}{4}$ goes away because $\frac{3D_q(t) - B_q(t)}{4} \approx D_q(t)$ on the left-hand side of (95). Taking the trace of (100), we find

$$\langle P_2 | (\Theta_q)_\alpha^\alpha | P_1 \rangle = \langle P_2 | \frac{T_R \alpha_s}{6\pi} F^2 | P_1 \rangle, \quad (102)$$

which is the correct trace anomaly relation to this order. To obtain (102), it is important to use the on-shell condition $p^2 = -t/4$ of the external states, so that the two terms in (100) contribute $\frac{1}{4}$ and $\frac{3}{4}$ of the total anomaly, respectively. Going from gluon to nucleon targets, we see that the way the trace anomaly relation (93) is fulfilled among various form factors is highly nontrivial. A different, spin-2 operator $F(D^+)^2 F$ is involved in the A_q, B_q form factor (98) due to the convolution integral in x . Moreover, a naive identification $p^\alpha p^\beta \rightarrow P^\alpha P^\beta$ is precarious because the nucleon is massive $P^2 = M^2 - t/4$. While the difference is negligible when $\sqrt{|t|} \gg M$, this obscures the fate of the poles in (98) as t gets smaller.

On the other hand, the tensor $l^\alpha l^\beta$ is formally identical for both the nucleon and the gluon targets, $l^\alpha = p_2^\alpha - p_1^\alpha = P_2^\alpha - P_1^\alpha$. We may therefore expect that the anomaly relation at the partonic level is better reflected in the $D_q(t)$ form factor even at the hadronic level, just as the $g_P(t)$ form factor which is the coefficient of l^α . Indeed, the opposite signs in (97) suggests that the pole terms mainly feed into the so-called Polyakov-Weiss D -term [49] of the unpolarized GPDs,

$$H_q^{\text{PW}}(x, \xi, t) = -E_q^{\text{PW}}(x, \xi, t) = \theta(\xi - |x|) D_q(x/\xi, t). \quad (103)$$

The distribution $D_q(z, t)$ is odd in z and is solely responsible for the highest power of ξ in the moments of GPDs. To extract it, we take the n th moment of (97) with odd integers n ,

$$\sum_q \int_{-1}^1 dx x^n H_q(x, \xi, t) \approx \frac{T_R n_f \alpha_s M^2}{\pi t} \int_0^1 dx \frac{x^n}{(n+2)(n+3)} \frac{1 - (\frac{\xi}{x})^{n+3}}{1 - \frac{\xi^2}{x^2}} (\mathcal{F}(x, \xi, t) - \mathcal{F}(x, \xi, 0)) \equiv \sum_{i=0}^{n+1} \sum_q h_{qn}^i \xi^i, \quad (104)$$

where we have minimally subtracted the pole at $t=0$ as in (89). The highest power h_{qn}^{n+1} is related to $D_q(z, t)$ as

$$\begin{aligned}
\sum_q \int_{-1}^1 dz z^n D_q(z, t) &\approx \sum_q h_{qn}^{n+1}(t) \\
&= \frac{T_R n_f \alpha_s M^2}{\pi t} \frac{1}{(n+2)(n+3)} \int_0^1 \frac{dx}{x} (\mathcal{F}(x, \xi, t) - \mathcal{F}(x, \xi, 0)) \\
&= -2 \frac{T_R n_f \alpha_s M}{\pi t} \frac{1}{(n+2)(n+3)} \left(\frac{\langle P_2 | F^2 | P_1 \rangle}{\bar{u}(P_2) u(P_1)} - \frac{\langle P_2 | F^2 | P_1 \rangle}{\bar{u}(P_2) u(P_1)} \Big|_{t=0} \right). \tag{105}
\end{aligned}$$

By definition, the $n = 1$ moment is the gravitational form factor $\int_{-1}^1 dz z D_q(z, t) = D_q(t)$. Inverting the Mellin transform (105) and noting that $D_q(z, t)$ is an odd function of z , we obtain

$$\sum_q D_q(z, t) \approx -\frac{T_R n_f \alpha_s}{\pi} z(1 - |z|) \frac{M}{t} \left(\frac{\langle P_2 | F^2 | P_1 \rangle}{\bar{u}(P_2) u(P_1)} - \frac{\langle P_2 | F^2 | P_1 \rangle}{\bar{u}(P_2) u(P_1)} \Big|_{t=0} \right), \tag{106}$$

and in particular,

$$\sum_q D_q(t) \approx -\frac{M}{t} \left(\frac{\langle P_2 | \frac{T_R n_f \alpha_s}{6\pi} F^2 | P_1 \rangle}{\bar{u}(P_2) u(P_1)} - \frac{\langle P_2 | \frac{T_R n_f \alpha_s}{6\pi} F^2 | P_1 \rangle}{\bar{u}(P_2) u(P_1)} \Big|_{t=0} \right). \tag{107}$$

Since $\langle P | F^2 | P \rangle < 0$ in QCD and the form factor $\langle P_2 | F^2 | P_1 \rangle$ is a decreasing function of $|t|$, the right-hand side of (106) is positive, whereas $D_q(t)$ is usually believed to be negative. While we expect that eventually the leading-order coefficient $\frac{T_R n_f \alpha_s}{6\pi}$ will be replaced by $\frac{\beta_q}{2g}$ after including higher-order corrections, according to the three-loop analyses in [45–47,50], the sign does not flip $\frac{\beta_q}{2g} > 0$. This suggests that the other terms in (95) that were neglected in the above minimal subtraction procedure may be numerically important as we already suspected in the argument below (85). Note also that the sign does flip if one includes the gluon contribution to recover the full beta function of QCD $\frac{\beta_q}{2g} \rightarrow \frac{\beta}{2g} < 0$.

VII. CONCLUSIONS

In this work, we have performed a complete one-loop calculation of the Compton scattering amplitude using momentum transfer t as the regulator of the collinear singularity. Our approach differs from all the previous calculations in the GPD literature where one typically uses dimensional regularization to isolate the collinear singularity and sets $t = 0$ right from the start, assuming that nonzero t only generates higher-twist corrections of order t/Q^2 . In practice, the introduction of an additional variable t makes the calculation more cumbersome and brings in unusual features. In the gluon initiated channel, we have found anomaly poles $1/t$ (29) and (30) accompanied by twist-four GPDs (9) and (10) in both the real and the imaginary parts of the Compton amplitude, confirming and

extending our previous finding [6]. In the quark initiated channel, we have unexpectedly found uncanceled single and double IR poles in the “coefficient functions” (25) and (26). Each of these features potentially implies the violation of factorization. However, we have also performed the one-loop calculation of GPDs for quark and gluon states with the same set of regulators and showed how all these poles can be systematically absorbed into the GPDs themselves. This shows that QCD factorization is restored at least to this order.

This is, however, not the end of the story. We have also explored connections between GPDs and anomalies as a natural and necessary consequence of the known connections between form factors and anomalies. We have argued that once the poles $1/t$ have been absorbed into GPDs, they become a part of the GPDs. In other words, anomalies nonperturbatively relate twist-two and twist-four GPDs. Such relations, once integrated over x , are expected to reproduce the constraints among the corresponding form factors. This scenario seems to be working for the polarized GPD \tilde{E}_q and its connection to the chiral anomaly. Relation (89), partly supported by the large- N_c argument, can be viewed as the x -dependent generalization of the form factor relation (77). The situation is more complicated (and more interesting) for the unpolarized GPDs H_q and E_q and their relation to the trace anomaly. We have argued that the anomaly mostly constrains the $D_q(t)$ form factor and its GPD analog, the Polyakov-Weiss D -term. The results we have arrived at in (106) and (107) are roughly consistent with the anomaly relation (95), but they differ in detail. Further investigation in this direction is necessary.

In conclusion, we have proposed finite- t regularization as an alternative factorization scheme that elucidates the physics of anomalies. This is a scheme where we are able to unravel novel connections between twist-two and twist-four GPDs mediated by the anomalies of QCD. Admittedly, the calculation is more cumbersome than the standard dimensional regularization with $t = 0$. Still, the chiral and trace anomalies are among the most fascinating phenomena of QCD with far-reaching consequences, and we believe that research on GPDs is enriched by incorporating such fundamental problems. There are a number of directions along which the current work can be refined or extended, in addition to the aforementioned tension between (95) and (107). First, we strongly suspect that anomaly poles are present in higher-order perturbation theory. Especially in the symmetric case, we expect that each additional loop provides the corresponding term in the expansion of the (quark part of the) beta function. A related question is whether there are anomaly poles in the *gluon* GPDs that complement the quark ones to restore the full beta function $\beta = \beta_q + \beta_g$ [44]. Another important question that has not been addressed at all in this paper is how to understand the new relations from a renormalization group point of view. In the present scheme, the mixing between the twist-two and twist-four GPDs occurs as a result of a finite subtraction rather than the DGLAP evolution of GPDs. The UV properties of the twist-four GPDs (9) and (10) have been studied in [19–22], but more work is certainly needed. Furthermore, it is well known that at twist-3 accuracy, the amplitude for DVCS off the nucleon contains twist-3 GPDs apart from the usual twist-2 GPDs. It is also interesting to pursue whether there are imprints of anomalies on twist-3 GPDs and related observables. Finally, constraints from anomalies should be implemented in the modeling of GPDs. In particular, the specific functional form given in (106) might be helpful to model this poorly constrained distribution.

ACKNOWLEDGMENTS

We are very grateful to Vladimir Braun and Anatoly Radyushkin for many useful discussions. We also thank Kornelija Passek-Kumerički, Swagato Mukherjee, Kazuhiro Tanaka, Raju Venugopalan, and Christian Weiss for discussions. S. B. and Y. H. are supported by the U.S. Department of Energy under Contract No. DE-SC0012704, and Laboratory Directed Research and Development (LDRD) funds from Brookhaven Science Associates. Y. H. is also supported by the framework of the Saturated Glue (SURGE) Topical Theory Collaboration. W. V. has been supported by Deutsche Forschungsgemeinschaft (DFG) through the Research Unit FOR 2926 (Project No. 409651613).

APPENDIX: DERIVATION OF EQ. (37)

In this appendix we give an outline of the derivation of (37) and (38). The other results in Sec. V can be derived similarly. For the quark matrix elements, we work in the Feynman gauge. The ladder diagram reads, up to a prefactor,

$$\mu^{2\epsilon} \int \frac{dk^- d^{2-2\epsilon}k_\perp}{(2\pi)^{3-2\epsilon}} \bar{u}(p+l/2) \frac{\gamma_\mu(\not{k} + \not{l}/2)\gamma^+(\not{k} - \not{l}/2)\gamma^\mu}{(p-k)^2(k-l/2)^2(k+l/2)^2} \times u(p-l/2), \quad (\text{A1})$$

where

$$k^+ = xp^+, \quad l^+ = -2\xi p^+, \quad l^- = -\frac{\xi l^2}{4p^+},$$

$$\vec{l}_\perp^2 = (\xi^2 - 1)l^2, \quad p^- = -\frac{l^2}{8p^+}. \quad (\text{A2})$$

In the DGLAP region $\xi < x < 1$, the k^- integral can be done by picking up the pole of $(p-k)^2 + i\epsilon = 0$ at

$$k^- = -\frac{k_\perp^2 + \frac{1-x}{4}l^2}{2(1-x)p^+}, \quad (\text{A3})$$

in the upper half-plane. The remaining propagators can be combined as

$$\frac{1}{1-x} \int_0^1 da \frac{A(k_\perp)}{(k^2 + (1-2a)k \cdot l + \frac{l^2}{4})^2}$$

$$= \frac{1-x}{(1-\xi(1-2a))^2} \int_0^1 da \frac{A\left(k'_\perp - \frac{(1-2a)(1-x)}{2(1-\xi(1-2a))}l_\perp\right)}{\left(k'^2_\perp - \frac{(1-a)a(1-x)^2l^2}{(1-\xi(1-2a))^2}\right)^2}, \quad (\text{A4})$$

where in the denominator we have shifted momentum $k_\perp \rightarrow k'_\perp$ to complete the square. In the numerator we have projected onto the twist-two component

$$\bar{u}(p+l/2) \cdots u(p-l/2) \rightarrow [(1-\epsilon)k'^2_\perp + (B-\epsilon C)l^2] \bar{u}\gamma^+u \equiv A\bar{u}\gamma^+u \quad (\text{A5})$$

with

$$B = \frac{(1-\xi + a(x+2\xi-1))(x-\xi-a(x-2\xi-1))}{(1-\xi(1-2a))^2},$$

$$C = \frac{(1-a)a(1-x)^2}{(1-\xi(1-2a))^2}. \quad (\text{A6})$$

The terms linear in k'_\perp have been dropped in (A5) since they vanish after the k'_\perp integral:

$$\begin{aligned} & \mu^{2\epsilon} \int_0^1 da \frac{1-x}{(1-\xi(1-2a))^2} \int \frac{d^{2-2\epsilon} k'_\perp}{(2\pi)^{2-2\epsilon}} \frac{(1-\epsilon)k'^2_\perp + (B-\epsilon C)l^2}{(k'^2_\perp - Cl^2)^2} \\ & \approx \left(\frac{\mu^2}{-l^2}\right)^\epsilon \int_0^1 da \frac{1-x}{(1-\xi(1-2a))^2} \frac{1}{(4\pi)^{1-\epsilon}} \left(\frac{(1-2\epsilon)\Gamma(\epsilon)}{C^\epsilon} - \frac{B\Gamma(1+\epsilon)}{C^{1+\epsilon}} \right). \end{aligned} \quad (\text{A7})$$

The first integral gives a UV pole:

$$\frac{\Gamma(\epsilon_{\text{UV}})}{4\pi} \left(\frac{4\pi\mu^2}{-l^2}\right)^\epsilon \int_0^1 da \frac{(1-x)(1-2\epsilon)}{(1-\xi(1-2a))^2 C^\epsilon} = \frac{1}{4\pi} \left(\frac{\tilde{\mu}^2}{-l^2}\right)^\epsilon \left(\frac{1}{\epsilon_{\text{UV}}} \frac{1-x}{1-\xi^2} - \frac{(1-x)(2\ln(1-x) - \ln(1-\xi^2))}{1-\xi^2} \right), \quad (\text{A8})$$

while the second integral gives double and single IR poles:

$$\begin{aligned} & \left(\frac{4\pi\mu^2}{-l^2}\right)^\epsilon \int_0^1 da \frac{1-x}{(1-\xi(1-2a))^2} \frac{-B\Gamma(1+\epsilon)}{C^{1+\epsilon}} \\ & = \left(\frac{\tilde{\mu}^2}{-l^2}\right)^\epsilon \frac{1}{(1-x)^{1+2\epsilon}} \left(\frac{2(x-\xi^2)}{1-\xi^2} \frac{1}{\epsilon_{\text{IR}}} - \frac{(1-x)^2 - 2(x-\xi^2)\ln(1-\xi^2)}{1-\xi^2} + \epsilon f(x) \right) \\ & = \left(\frac{\tilde{\mu}^2}{-l^2}\right)^\epsilon \left[-\delta(1-x) \left(\frac{1}{\epsilon_{\text{IR}}^2} + \frac{\ln(1-\xi^2)}{\epsilon_{\text{IR}}} \right) + \frac{2(x-\xi^2)}{(1-x)_+(1-\xi^2)} \frac{1}{\epsilon_{\text{IR}}} - \frac{4(x-\xi^2)}{1-\xi^2} \left(\frac{\ln(1-x)}{1-x} \right)_+ \right. \\ & \quad \left. - \frac{(1-x)^2 - 2(x-\xi^2)\ln(1-\xi^2)}{(1-\xi^2)(1-x)_+} - \frac{1}{2} \delta(1-x) \left(\ln^2(1-\xi^2) - \frac{\pi^2}{6} \right) \right]. \end{aligned} \quad (\text{A9})$$

Here $f(x)$ is a certain function whose value at $x=1$ is the only thing we need.

In Feynman gauge, there are two other diagrams, giving

$$\int \frac{d^d k}{(2\pi)^{d-1}} \bar{u}(p+l/2) \frac{\gamma^+ \not{k} \gamma^+ (\delta(k^+ - (x+\xi)p^+) - \delta((1-x)p^+))}{k^2(p-l/2-k)^2((1+\xi)p^+ - k^+)} u(p-l/2), \quad (\text{A10})$$

and the corresponding contribution for its mirror diagram. They can be similarly evaluated. The result is

$$\left(\frac{2(x-\xi^2)}{(1-\xi^2)(1-x)_+} + \delta(1-x)(2 - \ln(1-\xi^2)) \right) \left(\frac{\tilde{\mu}^2}{-l^2}\right)^\epsilon \left(\frac{1}{\epsilon_{\text{UV}}} - \frac{1}{\epsilon_{\text{IR}}} \right). \quad (\text{A11})$$

Adding also the quark self-energy diagrams on the external legs, we arrive at (37) and (38). We note that the calculation can also be performed in Landau gauge which has the advantage that the self-energy diagrams vanish identically.

In the ERBL region $\xi > x$, the pole of $(k+l/2)^2$ in (A1) moves to the upper half-plane. We thus pick up the pole of $(k-l/2)^2$ at

$$k_c^- = \frac{k_\perp^2 - (x\xi+1)\frac{l^2}{4} - \vec{k}_\perp \cdot \vec{l}_\perp}{2(x+\xi)p^+}, \quad (\text{A12})$$

in the lower half-plane. The first term in (A10) also contributes (but not its mirror diagram).

-
- [1] V. M. Braun, A. N. Manashov, S. Moch, and M. Strohmaier, *J. High Energy Phys.* **06** (2017) 037.
[2] V. M. Braun, A. N. Manashov, S. Moch, and J. Schoenleber, *J. High Energy Phys.* **09** (2020) 117; **02** (2022) 115(E).

- [3] V. M. Braun, Y. Ji, and J. Schoenleber, *Phys. Rev. Lett.* **129**, 172001 (2022).
[4] J. Schoenleber, *J. High Energy Phys.* **02** (2023) 207.
[5] R. Abdul Khalek *et al.*, *Nucl. Phys.* **A1026**, 122447 (2022).

- [6] S. Bhattacharya, Y. Hatta, and W. Vogelsang, *Phys. Rev. D* **107**, 014026 (2023).
- [7] A. Tarasov and R. Venugopalan, *Phys. Rev. D* **102**, 114022 (2020).
- [8] A. Tarasov and R. Venugopalan, *Phys. Rev. D* **105**, 014020 (2022).
- [9] X.-D. Ji and J. Osborne, *Phys. Rev. D* **58**, 094018 (1998).
- [10] A. V. Belitsky and D. Mueller, *Phys. Lett. B* **417**, 129 (1998).
- [11] L. Mankiewicz, G. Piller, E. Stein, M. Vanttinen, and T. Weigl, *Phys. Lett. B* **425**, 186 (1998); **461**, 423(E) (1999).
- [12] B. Pire, L. Szymanowski, and J. Wagner, *Phys. Rev. D* **83**, 034009 (2011).
- [13] V. Bertone, H. Dutrieux, C. Mezrag, J. M. Morgado, and H. Moutarde, *Eur. Phys. J. C* **82**, 888 (2022).
- [14] R. L. Jaffe and A. Manohar, *Phys. Lett. B* **223**, 218 (1989).
- [15] J. C. Collins and A. Freund, *Phys. Rev. D* **59**, 074009 (1999).
- [16] M. Diehl, *Phys. Rep.* **388**, 41 (2003).
- [17] A. V. Belitsky and A. V. Radyushkin, *Phys. Rep.* **418**, 1 (2005).
- [18] A. V. Radyushkin, *Phys. Rev. D* **58**, 114008 (1998).
- [19] Y. Hatta and Y. Zhao, *Phys. Rev. D* **102**, 034004 (2020).
- [20] Y. Hatta, *Phys. Rev. D* **102**, 094004 (2020).
- [21] A. Radyushkin and S. Zhao, *J. High Energy Phys.* **12** (2021) 010.
- [22] A. Radyushkin and S. Zhao, *J. High Energy Phys.* **02** (2022) 163.
- [23] H. H. Patel, *Comput. Phys. Commun.* **197**, 276 (2015).
- [24] G. 't Hooft and M. J. G. Veltman, *Nucl. Phys.* **B44**, 189 (1972).
- [25] P. Breitenlohner and D. Maison, *Commun. Math. Phys.* **52**, 11 (1977).
- [26] M. Jamin and M. E. Lautenbacher, *Comput. Phys. Commun.* **74**, 265 (1993).
- [27] A. Weber, *Nucl. Phys.* **B382**, 63 (1992).
- [28] W. Vogelsang, *Nucl. Phys.* **B475**, 47 (1996).
- [29] B. E. White, *J. Phys. G* **28**, 203 (2002).
- [30] G. Altarelli, R. K. Ellis, and G. Martinelli, *Nucl. Phys.* **B157**, 461 (1979).
- [31] M. Stratmann, A. Weber, and W. Vogelsang, *Phys. Rev. D* **53**, 138 (1996).
- [32] G. T. Bodwin and J.-W. Qiu, *Phys. Rev. D* **41**, 2755 (1990).
- [33] W. Vogelsang, *Z. Phys. C* **50**, 275 (1991).
- [34] M. Penttinen, M. V. Polyakov, and K. Goetze, *Phys. Rev. D* **62**, 014024 (2000).
- [35] E. Witten, *Nucl. Phys.* **B156**, 269 (1979).
- [36] G. Veneziano, *Nucl. Phys.* **B159**, 213 (1979).
- [37] M. Fujita, Y. Hatta, S. Sugimoto, and T. Ueda, *Prog. Theor. Exp. Phys.* **2022**, 093 (2022).
- [38] C. Cebulla, K. Goetze, J. Ossmann, and P. Schweitzer, *Nucl. Phys.* **A794**, 87 (2007).
- [39] X. Ji, *Front. Phys.* **16**, 64601 (2021).
- [40] K. A. Mamo and I. Zahed, *Phys. Rev. D* **103**, 094010 (2021).
- [41] D. E. Kharzeev, *Phys. Rev. D* **104**, 054015 (2021).
- [42] S. D. Bass, *Phys. Rev. D* **65**, 074025 (2002).
- [43] X.-D. Ji, *Phys. Rev. Lett.* **78**, 610 (1997).
- [44] Y. Hatta, A. Rajan, and K. Tanaka, *J. High Energy Phys.* **12** (2018) 008.
- [45] K. Tanaka, *J. High Energy Phys.* **01** (2019) 120.
- [46] T. Ahmed, L. Chen, and M. Czakon, *J. High Energy Phys.* **01** (2023) 077.
- [47] K. Tanaka, *J. High Energy Phys.* **03** (2023) 013.
- [48] M. Giannotti and E. Mottola, *Phys. Rev. D* **79**, 045014 (2009).
- [49] M. V. Polyakov and C. Weiss, *Phys. Rev. D* **60**, 114017 (1999).
- [50] A. Metz, B. Pasquini, and S. Rodini, *Phys. Rev. D* **102**, 114042 (2020).